

Strain-induced time reversal breaking and half quantum vortices near a putative superconducting tetracritical point in Sr_2RuO_4

Andrew C. Yuan ¹, Erez Berg,² and Steven A. Kivelson¹

¹*Department of Physics, Stanford University, Stanford, California 93405, USA*

²*Department of Condensed Matter Physics, Weizmann Institute of Science, Rehovot 7610001, Israel*



(Received 1 June 2021; accepted 20 July 2021; published 26 August 2021)

It has been shown that many seemingly contradictory experimental findings concerning the superconducting state in Sr_2RuO_4 can be accounted for as resulting from the existence of an assumed tetracritical point at near-ambient pressure at which $d_{x^2-y^2}$ and $g_{xy(x^2-y^2)}$ superconducting states are degenerate. We perform both a Landau-Ginzburg and a microscopic mean-field analysis of the effect of spatially varying strain on such a state. In the presence of finite xy shear strain, the superconducting state consists of two possible symmetry-related time-reversal symmetry (TRS) preserving states $d \pm g$. However, at domain walls between two such regions, TRS can be broken, resulting in a $d + ig$ state. More generally, we find that various natural patterns of spatially varying strain induce a rich variety of superconducting textures, including half-quantum fluxoids. These results may resolve some of the apparent inconsistencies between the theoretical proposal and various experimental observations, including the suggestive evidence of half-quantum vortices.

DOI: [10.1103/PhysRevB.104.054518](https://doi.org/10.1103/PhysRevB.104.054518)

I. INTRODUCTION

If it happens that superconducting (SC) orders with two distinct symmetries are comparably favorable for some microscopic reason, it is possible to have a two-parameter phase diagram (e.g., T and isotropic strain ϵ_0) that exhibits a multicritical point (e.g., at $\epsilon = \epsilon^*$ and $T = T^*$) at which the transition temperatures T_c of the two different orders coincide, as shown in Fig. 1(a). For instance, a change from s_{\pm} to d -wave pairing is thought to occur as a function of doping in certain Fe-based superconductors [1], and it was recently conjectured that the layered perovskite Sr_2RuO_4 (SRO) [2] under ambient conditions is “accidentally” close to such a multicritical point involving either $d_{x^2-y^2}$ and g -wave [3] or d_{xy} and s -wave [4,5] pairing. Even though both orders by themselves transform as one-dimensional irreducible representations (irreps) of the point-group symmetries, near such a multicritical point the system can exhibit a variety of features usually associated with a multicomponent SC order that transform according to a higher-dimensional irrep (e.g., a p -wave). Conversely, for a SC order parameter that transforms according to a two-dimensional (2D) irrep, the point of zero shear-strain, $\epsilon_{\text{shear}} = 0$, can be viewed as a special case of such a multicritical point in the T - ϵ_{shear} plane, as shown in Fig. 1(b). In both cases, the response of the different components of the SC order parameter to specific components of the strain tensor can produce a variety of novel effects.

Specifically, the proximity of a multicritical point implies that even small amplitude spatial variations of the strain field can locally stabilize different distinct forms of superconducting order in different domains. In this paper, we treat the case of a tetracritical point involving $d_{x^2-y^2}$ (B_{1g}) and $g_{xy(x^2-y^2)}$ -

wave (A_{2g}) pairing channels, where, as in Fig. 1(a), for the uniform case the coexistence regime is a $d + ig$ SC with spontaneously broken time-reversal-symmetry (TRS). We study this problem in the mean-field approximation, both from an effective field theory (Landau-Ginzburg/nonlinear sigma model) and a microscopic perspective. Following a similar line of reasoning as in Ref. [6] (where TRS breaking near dislocations was investigated), we show that inhomogeneous strain can lead to a highly inhomogeneous SC state in which TRS breaking is strongly manifest only along a network of domain walls separating regions in which the local strain favors one or another TRS preserving combination of the d and g order parameters. However, this only occurs when the unstrained system is close enough to the tetracritical point—in a sense that we make precise. We also show that appropriate strain patterns can induce an order parameter texture with a spontaneous fractional magnetic flux that equals a half superconducting flux quantum in under a range of circumstances.

The results we obtain are quite general as they follow largely from symmetry considerations. As an application of these ideas, we explore their implications for the still vexed problem of settling the symmetry of the superconducting state in SRO [2]. Here, there are a number of proposals, each of which can plausibly account for a subset of the experimental observations. Triplet pairing of any sort has seemingly been ruled out by recent nuclear magnetic resonance (NMR) experiments [7–9]. Moreover, recent ultra-sound measurements [10,11], taken at face value, require a two-component order parameter arising from the system in the absence of strain being accidentally tuned to a multicritical point involving d_{xy} and s or $d_{x^2-y^2}$ & g wave pairing. However, there are at least two sets of phenomena that seemingly challenge these theoretical proposals.

(1) Below a critical temperature T_{trsb} , the SC phase appears to break time-reversal symmetry [12–14] where at zero shear strain $T_{\text{trsb}} \approx T_c$, while in the presence of substantial B_{1g} shear strain these two transitions are split, such that $T_{\text{trsb}} < T_c$. However, specific heat measurements under the same circumstances show no signature of the TRS breaking transition [15,16]. An additional constraint on theory is the recent observation [17] that T_c can be depressed with the application of hydrostatic pressure (i.e., compressive uniform strain $\epsilon_0 < 0$) without producing a detectable splitting between T_c and T_{trsb} —an observation that was declared to rule out any theory based on an accidental degeneracy between two symmetry-distinct superconducting orders.

(2) A somewhat complicated experiment on mesoscale crystals adduced evidence of the existence of a topological excitation capable of admitting a half-quantum of magnetic flux [18]. This has been argued [19] to constitute direct evidence that the SC state is a chiral $p + ip$ state, despite the contrary evidence from the NMR studies [7–9]. Although additional evidence of half-quantum vortices has been recently reported [20], it is still possible that there is an alternative explanation for the observation that does not involve fractional vortices. However, taking the result at face value presents us with the need to identify a route to fractional vortices in a singlet SC.

In this context, our present results provide, as a matter of principle, possible routes to reconcile both these observations with the conjectured theoretical scenario.

(1) Despite the fact that the crystals involved in these experiments are paragons of crystalline perfection, the only plausible interpretation of the specific heat data is that the TRS breaking involves a small fraction of the electronic degrees of freedom. This can be naturally accounted for by the theoretically expected extreme sensitivity of the SC order to local strain, and the fact that the TRS breaking $d + ig$ order arises only in a network of domain-wall-like regions at which $|\epsilon_0 - \epsilon^*|$ and $|\epsilon_{\text{shear}}|$ are vanishingly small. Moreover, so long as the typical magnitude of the inhomogeneous strain is larger than an applied strain, no significant splitting between T_c and T_{trsb} is expected.

(2) The fact that a half-quantum vortex can be the ground state in the presence of a suitable strain texture similarly opens the possibility that the experimental evidence of fractional vortices in SRO is likewise consistent with the proposed scenario.

II. GINZBURG-LANDAU THEORY

A. Setup

We consider a Ginzburg-Landau free energy density [3] with order parameter (OP) fields $\Delta^T = (D, G)$ in the presence of an external magnetic field $\vec{B} = \vec{\nabla} \times \vec{A}$, given by

$$\begin{aligned} F &= V_2 + V_4 + K + \frac{B^2}{2}, \\ V_2 &= \alpha_0 \Delta^\dagger \Delta + \Delta^\dagger (\boldsymbol{\alpha} \cdot \boldsymbol{\tau}) \Delta, \\ V_4 &= \frac{1}{2} [\Delta^\dagger \Delta]^2 + \frac{\beta_1}{2} [\Delta^\dagger \tau_1 \Delta]^2 + \frac{\beta_3}{2} [\Delta^\dagger \tau_3 \Delta]^2 \\ &\quad + \frac{\beta'_3}{2} [\Delta^\dagger \tau_3 \Delta] [\Delta^\dagger \Delta], \end{aligned}$$

$$\begin{aligned} K &= \frac{\kappa}{2} |(-i\vec{\nabla} - \vec{A})\Delta|^2 \\ &\quad + \frac{\kappa'}{2} \{[(i\partial_x - A_x)\Delta^\dagger] \tau_1 [(-i\partial_y - A_y)\Delta] + \text{c.c.}\}, \end{aligned} \quad (1)$$

where $\boldsymbol{\tau}$ is the vector of Pauli matrices.

The complex scalar fields D, G are normalized so that the stiffness constants are equal, i.e., $\kappa_d = \kappa_g \equiv \kappa$, and that quartic isotropic coupling constant $\beta_0 = 1$. We used units such that the Cooper pair charge $2e = 1$. The quantity $\boldsymbol{\alpha} = (\alpha_1, 0, \alpha_3)$ represents the effect of local strain as a two-component vector, where $\alpha_3 = \alpha_3(x, y)$ is proportional to the deviation of the isotropic (A_{1g}) strain from its critical value ϵ_0^* and $\alpha_1 = \alpha_1(x, y)$ is proportional to the shear (B_{2g} , i.e., xy) strain. The free energy at $\vec{A} = \vec{0}$ respects TRS, has a $U(1)$ symmetry associated with the overall superconducting phase and, for $\alpha_1 = 0$, a D_{4h} point-group symmetry that involves both space and the order parameters. For example, under a rotation by $\pi/2$, $x \rightarrow y$ and $y \rightarrow -x$, $D \rightarrow -D$ and $G \rightarrow G$. The quartic terms determine the favored form of the ordered state: $\beta_3 > 0$ favors coexistence of nonzero d and g pairing and $\beta_1 > 0$ favors the TRS breaking combinations $d \pm ig$. The microscopic Bogoliubov–de Gennes (BdG) calculations reported in Sec. III A yield β_1 & $\beta_3 > 0$.

B. Nonlinear sigma model

In the special case, $\alpha_j = \beta_j = 0$ for all $j > 0$ and $\beta'_3 = 0$, $\kappa' = 0$, the free energy has a global $SU(2)$ symmetry that relates the two components of the order parameter. Not too close to T_c , (and to the extent that this symmetry is not too strongly broken, the variations of the magnitude of the order parameter are unimportant. This allows us to associate the relevant order parameter values with a point on a Bloch sphere $\hat{n} \in S^2$ via the isomorphism between $\mathbb{C}\mathbb{P}^1$ and $S^3/U(1)$, i.e.,

$$\begin{aligned} \Delta &= |\Delta| e^{i\chi} Z, \\ Z &= \begin{bmatrix} \cos(\frac{\theta}{2}) e^{-i\phi/2} \\ \sin(\frac{\theta}{2}) e^{+i\phi/2} \end{bmatrix}, \\ n_i &= Z^\dagger \tau_i Z. \end{aligned} \quad (2)$$

Here, defining χ_d and χ_g to be the phases of D and G respectively, $\chi = \frac{1}{2}[\chi_d + \chi_g]$ and $\phi = [\chi_g - \chi_d]$ are the overall and relative SC phases and $\theta = 2 \arctan[|G|/|D|]$. Note that OPs Δ which differ only by their global phases χ are mapped onto the same point on the Bloch sphere.

More generally, to the extent that it is possible to ignore variations in the magnitude of Δ , the problem reduces to a nonlinear sigma model with a weakly broken $U(1) \times SO(3)$ symmetry, derived in Appendix A

$$\begin{aligned} F &= K_\kappa + K_{\kappa'} + K_{\hat{n}} \\ &\quad + V_0(|\Delta|) + \tilde{\boldsymbol{\alpha}} \cdot \hat{n} + \frac{\tilde{\beta}_1}{2} [n_1]^2 + \frac{\tilde{\beta}_3}{2} [n_3]^2 + \dots, \\ K_\kappa &= \frac{\tilde{\kappa}}{2} |\vec{\nabla} \chi + \vec{a} - \vec{A}|^2, \\ K_{\kappa'} &= \tilde{\kappa}' n_1 \prod_{\mu=x,y} \left[\partial_\mu \chi + a_\mu - \frac{[\hat{n} \times \partial_\mu \hat{n}]_1}{2n_1} - A_\mu \right], \end{aligned}$$

$$K_{\hat{n}} = \frac{\tilde{\kappa}}{2} \left| \frac{\vec{\nabla} \hat{n}}{2} \right|^2 + \tilde{\kappa}' n_1 \left\{ \frac{[\hat{n} \times \partial_x \hat{n}]_1}{2n_1} \frac{[\hat{n} \times \partial_y \hat{n}]_1}{2n_1} - \frac{\partial_x \hat{n}}{2} \cdot \frac{\partial_y \hat{n}}{2} \right\}, \quad (3)$$

where $[\hat{n} \times \partial_\mu \hat{n}]_1 = n_2 \partial_\mu n_3 - n_3 \partial_\mu n_2$ is the first component of the vector $\hat{n} \times \partial_\mu \hat{n}$, while $\tilde{\kappa} \equiv |\Delta|^2 \kappa$, $\tilde{\alpha} \equiv |\Delta|^2 (\alpha_1, 0, \alpha_3 + \beta'_3 |\Delta|^2)$, $\tilde{\beta}_j \equiv |\Delta|^4 \beta_j$, and \dots signifies terms that would come from higher-order terms in the Ginzburg-Landau theory. Importantly, \vec{a} is the Berry connection associated with the motion of \hat{n} on the Bloch sphere

$$\vec{a} \equiv Z^\dagger \left(\frac{1}{i} \vec{\nabla} Z \right). \quad (4)$$

The corresponding Berry curvature is related to the Pontryagin density

$$\vec{\nabla} \times \vec{a} = \frac{1}{2} \epsilon_{\mu\nu} [\hat{n} \cdot (\partial_\mu \hat{n} \times \partial_\nu \hat{n})]. \quad (5)$$

C. Ground state

Let us first determine the ground state of a system in the presence of a uniform strain vector α using the Ginzburg-Landau free energy (1). For calculational convenience, we will consider the case $\beta'_3 = 0$ and $\beta_1 = \beta_3 = \beta > 0$ [in which case the free energy is invariant under a $U(1)$ symmetry associated with rotations of \hat{n} around n_2]. The general case is analyzed in Appendix B.

The potential term V of the Ginzburg-Landau free energy can be rewritten as a sum of two terms

$$V_2 = -|\Delta|^2 (\alpha_0 + \alpha \cdot \mathbf{m}), \\ V_4 = \frac{1}{2} |\Delta|^4 (1 + \beta m^2), \quad (6)$$

where \mathbf{m} is the projection of the normalized vector \hat{n} onto the \hat{e}_1 - \hat{e}_3 plane and $m \equiv |\mathbf{m}| = \sqrt{n_1^2 + n_3^2}$, where $n_j \equiv \hat{n} \cdot \hat{e}_j$. The potential is minimized when \mathbf{m} points in the same direction as α so that the potential term is given by

$$V = -|\Delta|^2 (\alpha_0 + \alpha m) + \frac{1}{2} |\Delta|^4 (1 + \beta m^2), \quad (7)$$

where $\alpha \equiv |\alpha|$. Since $0 \leq m \leq 1$, the values of $|\Delta|$ and m that minimize V are uniquely determined for $\alpha_0 \geq \alpha/\beta \geq 0$,

$$|\Delta|^2 = \alpha_0, \quad m = \frac{\alpha}{\beta \alpha_0}, \quad (8)$$

which corresponds to two distinct values \hat{n} (related by time-reversal symmetry) with $n_2 = \pm \sqrt{1 - m^2}$. For $\alpha/\beta > \alpha_0 \geq -\alpha$, we have

$$|\Delta|^2 = \frac{\alpha_0 + \alpha}{1 + \beta}, \quad m = 1, \quad (9)$$

so that $n_2 = 0$. Finally, $|\Delta| = 0$ for $\alpha < -\alpha_0$. Henceforth, we restrict our attention to the case $\alpha_0 > 0$ so $|\Delta| > 0$ and that the nature of the ground state is determined by the value of $\alpha/\beta \alpha_0$.

In the limit of small strain $\alpha \ll \beta \alpha_0$ so that $m \sim 0$, \hat{n} points in the $\pm \hat{e}_2$ direction, which corresponds to a TRSB $d \pm ig$ state. Conversely, if $\alpha \geq \beta \alpha_0$ so that $m = 1$, the Bloch vector \hat{n} points in the same direction as α as denoted by the solid black dot in Fig. 2. This corresponds to a TRS preserving state

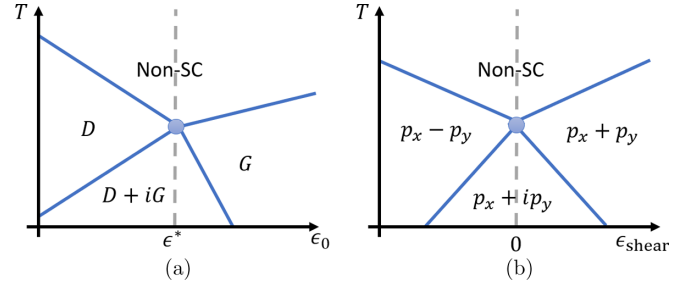


FIG. 1. (a) Schematic phase diagram as a function of two parameters—taken here to be isotropic strain (ϵ_0) and T , in the neighborhood of a tetracritical point at which the transition temperatures to SC states with d -wave (i.e., B_{1g}) and g -wave (i.e., A_{2g}) coincide. (b) A similar schematic phase diagram—now where the x -axis signifies symmetry breaking shear strain, ϵ_{shear} —for a system which at zero strain favors a SC order parameter the transforms according to a two-dimensional irrep., p_x and p_y (i.e., E_u symmetry). All figures are colored in the online version.

determined by the local strain. From now on, when we discuss a situation in which the strain is nonzero, we shall implicitly assume that $\alpha \geq \beta \alpha_0$ and thus the uniform ground state is as in Eq. (9).

D. Domain walls

We now consider the behavior of the order parameter Δ in the presence of spatially varying strain. As it simplifies the analysis, we will do this in the context of the nonlinear sigma model (3). To begin with, we consider a domain wall separating a region at $y < 0$ in which the shear strain favors $d - g$ pairing ($\alpha_1 < 0$) from a region at $y > 0$ that favors

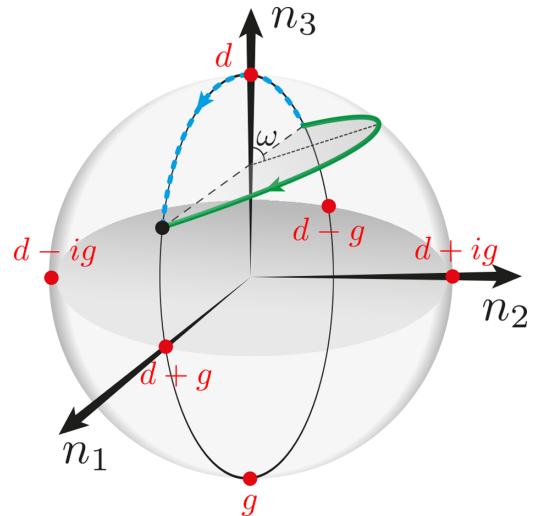


FIG. 2. Domain walls. The figure is the Bloch sphere representation of possible transitions across the domain wall where $\alpha_1(y) \rightarrow \pm \alpha_1$ as $y \rightarrow \pm \infty$, and $\alpha_3(y) \equiv \alpha_3 > 0$ is constant. The dashed blue arrow represents a TRS preserving transition through a pure d state. The solid green arrow represents a general TRSB transition restricted to a 2D plane intersecting the Bloch sphere, the angle of which relative to the \hat{e}_1 - \hat{e}_3 plane is denoted by ω . In particular, if $\omega = \pi/2$, then only the relative phase ϕ changes from $\phi = \pi \rightarrow 0$. All figures are colored in the online version.

$d + g$ ($\alpha_1 > 0$). We consider the system to be translationally invariant in the directions parallel to the domain wall.

Far from the domain wall, the relative phase $\phi(y)$ and amplitudes are determined by the strain. Thus, at long distances, the only property of the order parameter texture that can depend on the nature of the domain wall is the change in the global phase $\delta\chi$. If we choose the global phase such that the order parameter is real at $y \rightarrow -\infty$, across the domain wall the order parameter must change from $d - g$ to $e^{i\delta\chi}(d + g)$.

If TRS is preserved everywhere (i.e., if the order parameter can be chosen to be real), then the only possible values of $\delta\chi$ are 0 and π . Any other value of $\delta\chi$ requires TRSB on the domain wall, which consequently means that there must be two symmetry-related optimal values $\pm\delta\chi$.

Below we discuss the derivation of $\delta\chi$ in several cases. This is done by minimizing the free energy in Eq. (3) in the presence of a given strain texture. To be concrete, we will consider the case in which $\alpha_3(y) = \underline{\alpha}_3$ is a constant and $\alpha_1(y)$ changes sign across the domain wall such that $\alpha_1(y) \rightarrow \pm\underline{\alpha}_1$ as $y \rightarrow \pm\infty$ with $\underline{\alpha} > \beta\alpha_0$ [21]. The result can be expressed as a trajectory on the Bloch sphere, as shown in Fig. 2, where the arrow indicates the direction of evolution as y varies from $-\infty$ to $+\infty$.

To begin with, consider some general results that follow without explicit calculation.

(1) *Away from the multicritical point:* Consider the case in which $\underline{\alpha}_3 > \beta\alpha_0$. In this case, $|D|$ is everywhere larger than $|G|$ and even at the ‘‘center’’ of the domain wall, defined as the point $y = 0$ where $\alpha_1(0) = 0$, there is no local tendency to TRSB. The optimal order parameter texture lies in the \hat{e}_1 - \hat{e}_3 plane—as indicated by the dashed blue trajectory in Fig. 2. Here the G component of the order parameter vanishes at $y = 0$ and is negative on one side and positive on the other. Obviously, the analogous considerations apply for $\underline{\alpha}_3 < -\beta\alpha_0$, with the role of D and G interchanged. In this case, TRS is preserved everywhere and $\delta\chi = \pi$.

(2) *Broad domain wall near the multicritical point:* If $|\underline{\alpha}_3| < \beta\alpha_0$, then near the center of the domain wall, the local terms in the free energy favor a TRSB solution $d \pm ig$. Moreover, if the strain fields vary slowly on the scale of the superconducting coherence length, then the order parameter will be well approximated by the uniform state corresponding to the local value of the strain. Thus, the order parameter texture is not confined to the \hat{e}_1 - \hat{e}_3 plane, as shown by the solid green trajectory. This implies that both components of the order parameter remain nonzero everywhere, and thus that $\delta\phi = \delta\chi_g - \delta\chi_d = \pm\pi$. However, how much of this phase change is accommodated by changing the phase of D or G depends on energetics; if the D wave order is everywhere dominant, then $\delta\chi_d \approx 0$ and hence $\delta\chi \approx \pi/2$, while if the D and G are of nearly equal strength, then $|\delta\chi_g| \approx |\delta\chi_d|$ and hence $\delta\chi \approx 0$. Clearly, for intermediate cases, $0 < |\delta\chi| < \pi/2$.

(3) *Narrow domain wall near the multicritical point:* Here, the nature of the solution depends on a host of microscopic details. Since ‘‘narrow’’ and ‘‘broad’’ refer to the width of the domain wall relative to the superconducting coherence length, and given that the superconducting coherence length diverges as $T \rightarrow T_c$, at least near T_c this is likely the most physically relevant situation. We will thus treat this case more explicitly below.

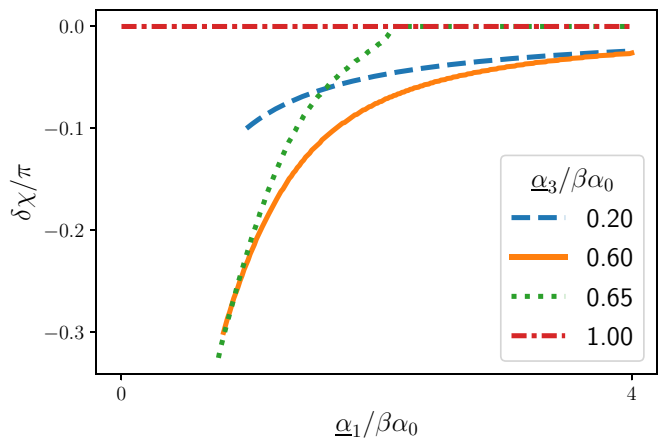


FIG. 3. Global phase. The change $\delta\chi$ in the global phase across a narrow domain wall where the xy component of the strain α_1 is discontinuous. The domain wall is characterized by $\alpha_1(y) = \underline{\alpha}_1 \text{sign}(y)$, while $\alpha_3(y) = \underline{\alpha}_3$ is constant. $\delta\chi$ is shown as a function of $\underline{\alpha}_1/\beta\alpha_0$. The different curves correspond to different fixed values of the uniform component of the strain, $\underline{\alpha}_3/\beta\alpha_0$. All figures are colored in the online version.

As an explicit model of a narrow domain wall, let $\alpha_1(\vec{r}) = \underline{\alpha}_1 \text{sign}(y)$ where $\underline{\alpha}_1 > 0$ and $\alpha_3(\vec{r}) \equiv \underline{\alpha}_3 \geq 0$ be a constant. We consider paths in which as y goes from $-\infty$ to $+\infty$, $\hat{n}(y)$ follows a trajectory that lies in a plane ω intersecting the Bloch sphere—of the sorts illustrated by the different colored paths in Fig. 2. When this plane is perpendicular to \hat{e}_2 , TRS is preserved (dashed blue line) while all other trajectories break TRS. A more complete solution of the problem does not result in qualitative changes in the conclusions. With these simplifications, the domain wall energies ΔF can be computed analytically (see Appendix C).

We can then find the plane ω with minimum domain wall energy for each set of values $\underline{\alpha}_1, \underline{\alpha}_3$ and compute the corresponding change in global phase $\delta\chi$, as shown in Fig. 3. For $\underline{\alpha}_3 \geq \beta\alpha_0$ (i.e., away from the multicritical point), TRS is preserved everywhere, such that $\delta\chi = 0$. Conversely, if $\underline{\alpha}_3 < \beta\alpha_0$, (near the multicritical point), TRS breaking near the domain wall is possible, yielding $0 < |\delta\chi| < \pi/2$.

E. Topological point defects

The domain walls we discussed are natural strain patterns that are plausibly generic in real materials. In addition, because there are two components of the strain-dependent vector α , one can also conceive of vortex-like defects with point-like cores in two dimensions or line-like cores in three dimensions. Here, we consider a pattern of strain such that along any path encircling the origin, $\alpha(\vec{r})$ rotates by 2π . Given such a strain pattern, we can use the nonlinear sigma model to explore the properties of the resulting SC order parameter texture that results.

1. Vorticity and associated flux

Far from the defect core, the form of the SC order parameter (up to its overall phase) is essentially determined by the local pattern of strain. Regardless the SC order parameter

texture, the current density $\vec{J} = -\delta F/\delta \vec{A}$ can be computed exactly from the nonlinear sigma model (3) since variations in magnitude $|\Delta|$ do not couple to the vector potential \vec{A} . From this it follows that

$$J_x = \tilde{\kappa}[\partial_x \chi + a_x - A_x] + \tilde{\kappa}' n_1 \left[\partial_y \chi + a_y - \frac{[\hat{n} \times \partial_y \hat{n}]_1}{2n_1} - A_y \right] \quad (10)$$

and similarly for J_y . Far from the core under most circumstances $\vec{J} \rightarrow \vec{0}$; indeed, beyond a London penetration depth it vanishes exponentially. Thus, we can invert Eq. (10) to obtain an expression for \vec{A} in terms of the SC order parameter texture valid wherever \vec{J} is negligible. Then, by integrating the vector potential \vec{A} along a contour C that encloses the origin at a distance, we obtain an expression (modulo an additive integer) for the enclosed flux Φ in units of the superconducting flux quantum $\Phi_0 = h/2e$:

$$\frac{\Phi}{\Phi_0} = \frac{\Omega}{4\pi} - \frac{\kappa'}{4\pi} \oint_C [\hat{n} \times \partial_\mu \hat{n}]_1 T_{\mu\nu} dr_\nu, \quad T = \begin{bmatrix} \kappa' n_1 & \kappa \\ \kappa & \kappa' n_1 \end{bmatrix}^{-1}, \quad (11)$$

where Ω is the solid angle enclosed by the contour of \hat{n} on the Bloch sphere.

Note that when $[\hat{n} \times \partial_\mu \hat{n}]_1 = 0$ along C , the second term vanishes and thus the flux quantum captured is expressed entirely in terms of the Berry phase $\Omega/4\pi$. In particular, since strain stabilizes a TRS preserving state, we will typically be interested in situations in which $\hat{n} \cdot \hat{e}_2 = 0$ far from the defect core, insuring that this condition is satisfied. In this case, whenever \hat{n} follows a trajectory that encircles the origin [as in Fig. 4(b)], there must be an associated half-flux quantum of flux bound to the defect.

2. Example of a strain-induced half-quantum fluxoid

We now consider an explicit version of such a strain texture [Fig. 4(a)], consisting of four domains separated by domain walls that intersect at the origin. Thus, we take $\alpha_3(x, y) = \alpha_3 F_3(x)$ and $\alpha_1(x, y) = \alpha_1 F_1(y)$, where $F_j(r) = -F_j(-r)$, and $F_j(r) \rightarrow 1$ as $r \rightarrow \infty$. We further assume that $\alpha_j > \beta\alpha_0$, i.e., far away from the origin we are in the large strain regime where the preferred order parameter is set by the strain and TRS is preserved. As indicated by the labels, the D component is enhanced compared the G component for $x > 0$. For $x < 0$, the G component is favored. The combination $d + g$ is favored for $y > 0$, while $d - g$ is favored for $y < 0$.

Let us now consider a closed path C encircling the origin [Fig. 4(a)], where the preferred SC state (up to the global phase) is denoted in each quadrant, e.g., $D + g$ denotes a TRS preserving SC state with dominant D component. Since the contour C is far away from the origin, the domain walls between quadrants are narrow, and the strain is always sufficiently large such that TRS breaking is never favored locally. Figure 4(b) shows the trajectory of the order parameter on the Bloch sphere, in which each segment of the contour is color/style-coded to correspond to that in the top diagram. We then see that the OP Δ wraps around by 2π while being

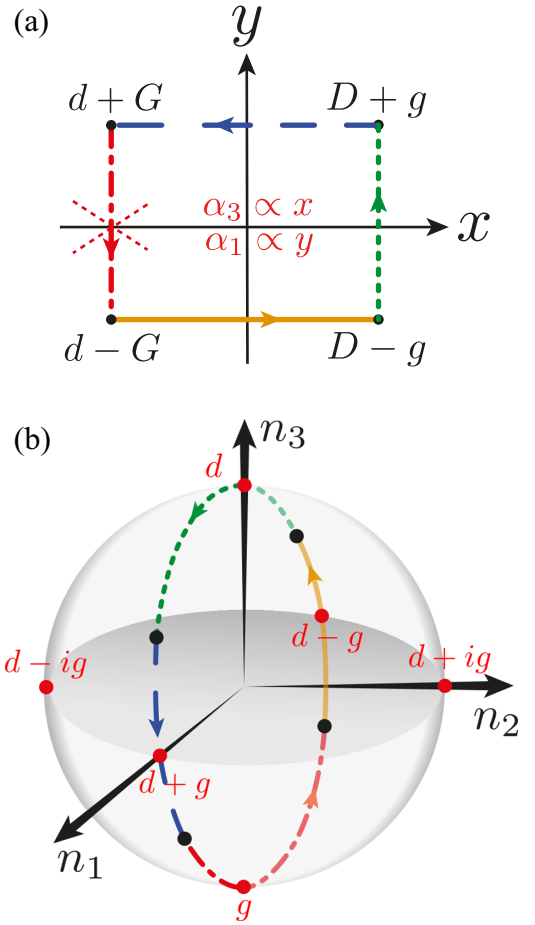


FIG. 4. A strain induced half quantum fluxoid. (a) Real-space contour around a topological point defect, along which the strain vector α winds by 2π . The dashed cross shows the location of a π mismatch in the phase of the order parameter. $D + g$ in the $x > 0$, $y > 0$ quadrant represents order parameter with a dominant D component and a smaller G component, and similarly in the other quadrants. (b) Corresponding trajectory of the order superconducting order parameter along the Bloch sphere. TRS is preserved along the path. Each segment of the contour is color/style-coded so that the same colors/line styles in the bottom and top figure correspond to each other. All figures are colored in the online version.

confined to the \hat{e}_1 - \hat{e}_3 plane and thus $[\hat{n} \times \partial_\mu \hat{n}]_1 = 0$ along the contour. Eq. (11) thus implies that this strain texture captures a half quantum of flux.

At an intuitive level, the same conclusion can be reached by considering the nature of the order parameter texture along the various line segments in Fig. 4(a). Since it is energetically favorable to keep the dominant piece of the SC order parameter uniform, the overall phase ($\delta\chi$) is constant along any of the segments other than the red one (dashed cross), along which the dominant portion of the order parameter changes sign, favoring $\delta\chi = \pi$. Of course, this change in phase will in actuality be spread out along the entire path, but this argument captures the π phase mismatch along the close path that results in a half-quantum vortex.

III. MICROSCOPIC ANALYSIS

We now address these same issues from a more microscopic perspective in the context of Bardeen-Cooper-Schrieffer (BCS) mean-field theory. Specifically, we solve the self-consistency equations for a generic 2D Hamiltonian with attractive d - and g -wave interactions, and with spatially varying band-structure parameters that encode the same patterns of spatially varying strain discussed above.

Let the full Hamiltonian $H_{\text{full}} = H_0 + H_1$ be defined on a 2D square lattice. The free Hamiltonian H_0 is characterized by the (single-band) TRS-preserving hopping matrix t so that

$$H_0 = - \sum_{\vec{r}', \vec{r}, s} [t(\vec{r}', \vec{r}) + \mu] c_{\vec{r}'s}^\dagger c_{\vec{r}s} \quad (12)$$

and the attractive (pairing) interaction term H_1 , assumed to be spatially uniform, is

$$H_1 = - \sum_{\tau=d,g} \lambda_\tau \sum_{\vec{r}} P_\tau^\dagger(\vec{r}) P_\tau(\vec{r}),$$

$$P_\tau^\dagger(\vec{r}) = \sum_{\vec{r}', s, s'} f_\tau(\vec{r}' - \vec{r}) c_{\vec{r}'s'}^\dagger [i\sigma_2]_{s's} c_{\vec{r}s}^\dagger, \quad (13)$$

where $\lambda_\tau > 0$ with $\tau = d$ or g encodes the strength of the interaction in the designated symmetry channels. Here f_τ are TRS preserving form factors that transform according to the requisite distinct irreducible representations of the point-group symmetry

$$f_d(\vec{r}) = \frac{1}{4} \delta(r=1)[x^2 - y^2],$$

$$f_g(\vec{r}) = \frac{3\sqrt{3}}{32} \delta(r=\sqrt{5})[xy(x^2 - y^2)], \quad (14)$$

where the factor of the Kronecker- δ in each expression is 1 when \vec{r} connects, respectively, first and fourth nearest-neighbor sites. The hopping matrix elements can likewise be expressed in terms of these and the local strain as

$$t(\vec{r} + \vec{r}', \vec{r}) = \delta(r' = 1) + t\delta(r' = \sqrt{2})$$

$$+ g_s(\vec{r}) \odot f_s(\vec{r}') + g_{d'}(\vec{r}) \odot f_{d'}(\vec{r}'), \quad (15)$$

where $g_s(\vec{r})$ and $g_{d'}(\vec{r})$ parametrize, respectively, the spatial profile of the isotropic and shear strain, and \odot is the symmetrization of the product term, e.g., $g_s(\vec{r}) \odot f_s(\vec{r}') \equiv \frac{1}{2}[g_s(\vec{r}) + g_s(\vec{r} + \vec{r}')]f_s(\vec{r}')$. Here, $f_s(\vec{r})$ and $f_{d'}(\vec{r})$ are form factors with isotropic and shear $[xy]$ symmetry of the underlying lattice, which we take to be

$$f_s(\vec{r}) = \delta(r=2), \quad f_{d'}(\vec{r}) = \delta(r=\sqrt{2})[xy]. \quad (16)$$

We construct a mean-field BCS trial Hamiltonian H , given by

$$H = \sum_{\vec{r}', \vec{r}, s} \mathcal{T}(\vec{r}, \vec{r}) c_{\vec{r}s}^\dagger c_{\vec{r}s} + \sum_{\vec{r}', \vec{r}} [\Delta(\vec{r}', \vec{r}) c_{\vec{r}'\uparrow}^\dagger c_{\vec{r}\downarrow}^\dagger + \text{H.c.}] \quad (17)$$

The full self-consistency field equations (SCFs) can then be derived by extremizing the resulting variational free energy in the standard fashion—details are given in Appendix D. It should be noted that in order to guarantee that the results satisfy the equation of continuity, i.e., $\vec{\nabla} \cdot \vec{J} = 0$, it is generally

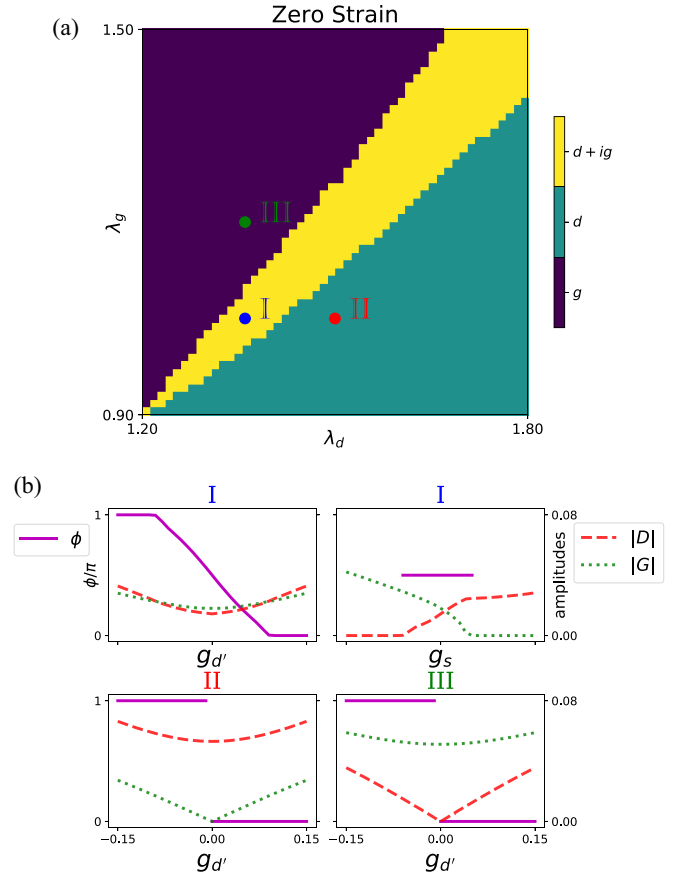


FIG. 5. (a) Phase diagram of the microscopic Hamiltonian, Eqs. (12) and (13), as a function of the interaction strengths λ_d, λ_g , calculated within self-consistent mean-field theory, in the absence of strain. Near degeneracy $\lambda_d \sim \lambda_g$, the middle portion denotes the TRSB $d + ig$ state, while the bottom and top regions represent a pure d and pure g state, respectively. Three representative points (I, II, III), one in each phase, are used in further calculations. (b) The top two panels depict the evolution of the uniform state at point (I) with shear $g_{d'}$ and isotropic g_s strain. The solid line represents the relative phase ϕ given by the left y-axis, while the dashed lines represent the amplitudes $|D|, |G|$, given by the right y-axis. Similarly, the bottom two panels represent the evolution of the uniform state for sample points (II) and (III) under shear $g_{d'}$ strain. All figures are colored in the online version.

insufficient to only solve the SCFs for the gap function—both \mathcal{T} and Δ must be determined self-consistently (see Appendix E for a proof).

A. Uniform states

To begin with, we study the uniform case tuned close to the multicritical point. In Fig. 5(a) we show the mean-field ground-state phase diagram of the microscopic model defined above as a function of the pairing interactions, λ_d and λ_g , in the absence of “strain” (i.e., for $g_s = g_{d'} = 0$), for $t = 0.4$ and for the chemical μ chosen so that the mean electron density per site is $n \approx 0.3$. There are three distinct phases in this case: a pure d wave phase for λ_d sufficiently larger than λ_g , a pure g wave phase for sufficiently large λ_d , and a relatively narrow coexistence phase centered at the line $\lambda_d = \lambda_g$. The later phase

has a relative phase $\phi = \pm\pi/2$, i.e., it is a $d \pm ig$ phase, for all parameters studied here.

To illustrate the effect of shear strain, we chose representative points in the phase diagram indicated by the three points in Fig. 5(a), and explore the evolution of the ground-state order upon application of uniform strain, i.e., nonzero g_d' or g_s . Shown in Fig. 5(b) are the magnitude of the d and g components of the order parameter, $|D|$ and $|G|$, as well as the relative phase, ϕ , for these three cases as follows.

(1) The top two panels of Fig. 5(b) show the evolution with strain of the case in which we are most interested—the strain-free ground state has $d \pm ig$ pairing. As the shear strain g_d' is varied, $|D|$ and $|G|$ remain comparable, although both increase slightly, roughly in proportion to $|g_d'|^2$ —which is a density of states effect. More dramatically, the relative phase evolves smoothly, up to a critical value at which TRS is restored, i.e., where ϕ reaches either 0 or π , which marks the point of a transition to $d + g$ or $d - g$ pairing, respectively. In contrast, as a function of the isotropic strain g_s , the evolution from the $d + ig$ state to a pure g or pure d state involves a change of the relative amplitudes $|D|$ and $|G|$, while the relative phase $\phi = \pm\pi/2$ remains constant.

(2) The lower two of Fig. 5(b) represent the shear strain evolution under conditions in which at zero strain either the d or g component is absent. In both cases, the component that is dominant at zero strain remains dominant; indeed, its overall magnitude increases in much the same way as in the top panel. As required by symmetry, the component that vanished in the absence of strain exhibits an initial linear increase in magnitude with increasing strain. However, in this case, the relative phase is a discontinuous function of strain; the ground-state always preserves TRS and jumps from being $d + g$ to $d - g$ as the sign of the strain changes.

We relate these results to the Ginzburg-Landau theory as follows: In the absence of strain, the system is tuned to the tricritical condition $\alpha_1 \approx \alpha_3 \approx 0$ when $\lambda_d \approx \lambda_g$. Moreover, since the system exhibits $d + ig$ order in this case, the requisite inequalities $\beta_1 > 0$, $\beta_3 > 0$ are automatically satisfied. The shear strain can be identified with $\alpha_1 \propto g_d'$. Conversely, even relatively small values of $|\lambda_d - \lambda_g|/|\lambda_d + \lambda_g| > 0.1$ are enough to produce a sufficiently large value of α_3 such that even at $T = 0$, $|\alpha| > \beta/|\alpha_0|$. Also notice that we have taken relatively strong interactions; this condition becomes exponentially more restrictive the weaker the overall coupling $|\lambda_d + \lambda_g|$. The extent to which the system needs to be “fine-tuned” near to the tetracritical point is quantified as the narrowness of this coexistence phase in the zero-temperature phase diagram.

B. Domain walls

We next address the domain wall behavior for a system near and away from the multicritical point. To circumvent the difficulty of large coherence lengths at small interaction strength, we use large interaction strengths $\lambda_d = 3.2$ and $\lambda_g = 4.9$, chosen such that in the absence of strain, the uniform system is near the multicritical point, i.e., in a $d + ig$ state. We then introduce an x -dependent shear strain with a domain wall along the y -axis, along which the system is translationally

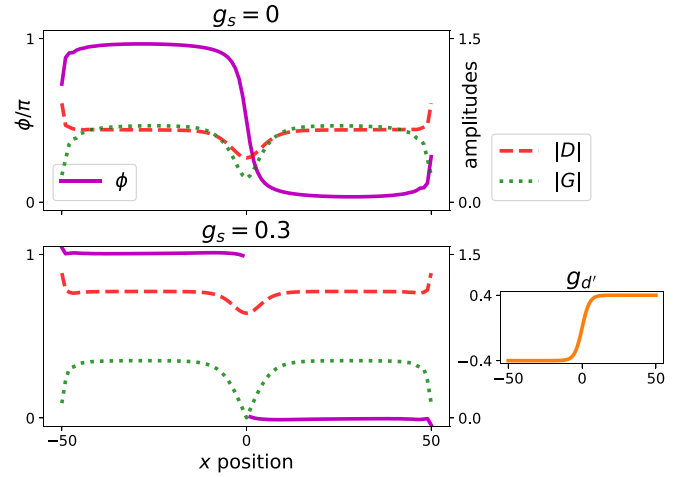


FIG. 6. Domain walls. The top panel shows the behavior of the SC order parameter across a domain wall at which the shear strain $g_d'(x)$ changes sign when the system is detuned from the multicritical point such that $g_s(x) = 0.3$. The bottom panel shows the same sort of domain wall for a system near the multicritical point so that $g_s(x) = 0$. The spatial variation of g_d' , shown in the mini-plot, is of the form $g_d'(x) = 0.4 \tanh(x/l)$ where $l = 5$ and $|x| \leq L = 50$. The solid line represents the relative phase ϕ with values given by the left y-axis, while the dashed lines are the amplitudes of the D and G components with values given by the right y-axis. All figures are colored in the online version.

invariant. As a specific example, we take $g_d' = 0.4 \tanh(x/l)$ where $l = 5$ and $|x| \leq L = 50$. We take $g_s(x)$ to be constant.

Figure 6 (top) shows the profiles of the order parameters and relative phase ϕ as a function of x in the case $g_s = 0$, i.e., near the multicritical point. ϕ twists through $\pi/2$ passing through the domain wall, indicating the TRS is broken there. Figure 6 (bottom) shows a TRS preserving domain wall for $g_s = 0.3$, i.e., away from the multicritical point.

C. Half-quantum vortex

Finally, to construct a tractable situation in which the previously discussed phenomenological analysis leads to a half-quantum vortex, we consider the previous system on an infinite cylinder with periodic boundary conditions in the x -direction and translational invariance along the y -direction. The circumference of the cylinder (in the x -direction) is 400 sites. We then vary the microscopic terms [$g_s(x)$ and $g_d'(x)$] corresponding the evolution of α_1 and α_3 shown in Fig. 4. Solving the full SCF equations, we obtain $D(x)$ and $G(x)$ as shown in Fig. 7.

The results corroborate the expected behavior from the Ginzburg-Landau theory. Notice that the x -labels on top of Fig. 7(a) indicate the expected state at each position along the contour. Most importantly, the relative phase ϕ winds by 2π around the cylinder, from which it follows that $\delta\chi = \pi$. This result is translated into a trajectory on the Bloch sphere in Fig. 7(b). Note that the trajectory of the order parameter is close to the \hat{e}_1 - \hat{e}_3 plane, but deviates from it somewhat in parts of the trajectory, indicating that TRS is broken in certain regions along the path. Correspondingly, in this calculation, we

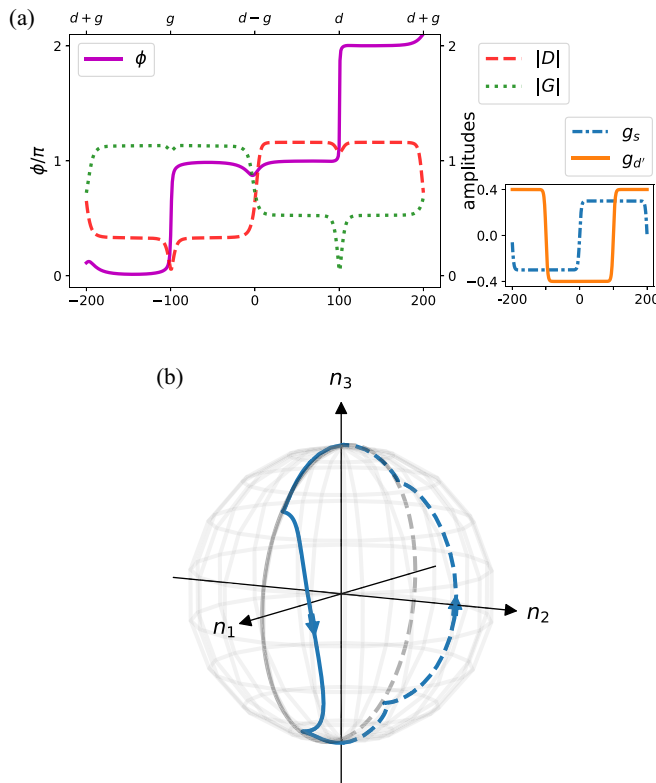


FIG. 7. Half-quantum vortex pinned by strain texture. (a) The behavior of the OP $\Delta = (D, G)$ as a function of x . The two components of the strain, $g_s(x) \propto \alpha_3$ and $g_d(x) \propto \alpha_1$, are shown on the right. The domain walls are of the form $\pm \tanh(x/l)$ with $l = 5$, and the cylinder's circumference is 400 sites. The solid line represents the relative phase ϕ given by the left vertical axis, while the dashed lines represent that amplitudes $|D|$ and $|G|$ (right vertical axis). The bottom horizontal axis represents the x position, while the top horizontal axis is labeled with the uniform state corresponding to the given strain texture at that position. (b) Trajectory of the OP $\Delta = (D, G)$ projected onto the unit Bloch sphere. The arrow represent the direction of the contour. The gray circle line emphasizes the \hat{e}_1 - \hat{e}_3 plane. All figures are colored in the online version.

expect the flux induced by the strain pattern to deviate slightly from $\Phi_0/2$ [see Eq. (11) and the discussion that follows].

IV. CONCLUSION

In this paper we primarily explored the effect of inhomogeneous strain on the superconducting OP textures of a system tuned close to a tetracritical point at which two different superconducting components have equal T_c 's. Such a tetracritical point can arise due to symmetry—when in the absence of strain the two components form a two-dimensional irreducible representation of the point group symmetries. However, we have primarily focused on the case in which the tetracritical point arises from tuning a symmetry preserving parameter near to a critical value—a situation that might arise accidentally in a small subset of superconducting materials.

In this situation, even relatively small local strain can readily detune the system from the tetracritical condition sufficiently that a single component OP is locally favored.

However, if on average the system is near enough to this critical value, it is also natural to find domain walls between regions of different dominant strain in which the system is approximately tetracritical. This, in turn, can lead to TRS breaking on such domain walls, and thus to a state which globally breaks TRS but in which the symmetry breaking is locally significant only on a network of such domain walls. We also showed that appropriate patterns of inhomogeneous strain can bind a half-quantum vortex.

These results may have interesting implications for a number of materials that show evidence for either an exact or a near-degeneracy of two SC orders, including UPt_3 [22–24], URu_2Si_2 [25,26], UTe_2 [27], doped Bi_2Se_3 [28,29], certain Fe-based superconductors [30–32], and of course SRO. Most importantly, such a near degeneracy necessarily implies an enhanced sensitivity to variations in local strain, which can lead to a variety of otherwise unexpected behaviors. Note, however, that half-quantum vortices and other topological defects can also arise as dynamical excitations in multicomponent superconductors in the absence of any strain effects [33–39].

It is worth noting that while our results are quite general, they are obtained within mean-field theory, and neglect thermal fluctuations of the superconducting order parameter. These can lead to interesting effects close to the T_c in multicomponent superconductors [40–43].

This study was undertaken with the SC state of SRO in mind. It is well established that the SC state is highly strain-sensitive. There are also a variety of experimental observations—ultra-sound anomalies key among them—that are most naturally consistent with an assumed near degeneracy between a d and g wave SC component. However, a variety of other experimental results appear, at first, difficult to reconcile with this scenario [14,17,18,44]. The present results suggest a route to understanding some of these additional observations. This includes a suppressed thermodynamic signature of the TRS breaking transition and the possibility of half-quantum vortices, even though some aspects of the actual experiment [18]—for instance the dependence on an in-plane field—still need be addressed.

As mentioned in the Introduction, a key issue concerns the strain-induced splitting between the SC and the TRS breaking transitions. It has been found that $x^2 - y^2$ (B_{1g}) shear strain can produce a significant increase in T_c , with a small decrease in T_{trsb} [15]—i.e., a split transition—while hydrostatic pressure (which produces A_{1g} strain) can produce a pronounced depression of T_c but no detectable splitting of the transition [17]. These observations are trivially accounted for if one assumes that α_3 has a strong (albeit quadratic) dependence on shear strain but only weakly dependent on isotropic strain while α_0 depends on both components of the strain.

How stringent a condition this places on the isotropic strain dependence of α_3 depends on the magnitude and character of the strain inhomogeneities, i.e., the width of the SC transition. To the extent that we can ignore the effect of xy (B_{2g}) shear strain (i.e., for $\alpha_1 \approx 0$), it follows that so long as there are regions of d and regions of g wave SC, there must be domain walls between them at which TRS breaking can arise. Thus, a split transition will be apparent only when the mean value of α_3 is greater than its variance.

The present considerations are encouraging in the sense that they illustrate a plausible explanation of a set of previously puzzling experiments in SRO. However, it is important to reiterate that this analysis sheds no insight of what is probably the most vexing aspect of the proposed scenario: why are these two symmetry distinct forms of SC order nearly degenerate with one another without need of any fine-tuning?

ACKNOWLEDGMENTS

We acknowledge extremely helpful discussions with Clifford Hicks, Catherine Kallin, Tony Leggett, Andy MacKenzie, and Brad Ramshaw. S.A.K. and A.C.Y. were supported, in part, by NSF Grant No. DMR-2000987 at Stanford. E.B. was supported by the European Research Council (ERC) under grant HQMAT (Grant Agreement No. 817799), the Israel-US Binational Science Foundation (BSF), and a Research grant from Irving and Cherna Moskowitz.

APPENDIX A: DERIVATION OF NONLINEAR SIGMA MODEL

Here, we review an efficient method of deriving the nonlinear sigma model in Eq. (3). Suppose that the OP $\Delta = \Delta(q)$ depends smoothly on parameter q . Then its change $\Delta(q) \rightarrow \Delta(q + \delta q)$ can be expressed as an infinitesimal rotation along with a change in the Berry phase γ , i.e.,

$$\Delta(q + \delta q) = e^{i\delta\gamma} U(q)^{\delta q} \Delta(q), \quad (\text{A1})$$

where $U(q)^{\delta q} \equiv \exp[-iH(q)\delta q] \in SU(2)$ is the infinitesimal rotation with

$$H(q)\delta q = \frac{1}{2}(\hat{\mathbf{n}} \times \delta\hat{\mathbf{n}}) \cdot \boldsymbol{\tau}. \quad (\text{A2})$$

Therefore, we can write

$$(-i\partial_\mu - A_\mu)\Delta = (\partial_\mu\chi + a_\mu - A_\mu - H_\mu)\Delta, \quad (\text{A3})$$

$$H_\mu = \frac{1}{2}(\hat{\mathbf{n}} \times \partial_\mu\hat{\mathbf{n}}) \cdot \boldsymbol{\tau}. \quad (\text{A4})$$

Using the (anti)commutation relations of the Pauli matrices, we can then efficiently derive the nonlinear sigma model, e.g.,

$$\Delta^\dagger H_\mu^2 \Delta = \frac{|\Delta|^2}{2} \text{tr}[H_\mu^2(\tau_0 + \hat{\mathbf{n}} \cdot \boldsymbol{\tau})] \quad (\text{A5})$$

$$= |\Delta|^2 \left| \frac{\partial_\mu \hat{\mathbf{n}}}{2} \right|^2. \quad (\text{A6})$$

Similarly, we have

$$\Delta^\dagger H_\mu \Delta = 0, \quad (\text{A7})$$

$$\text{Re}[\Delta^\dagger H_x \tau_1 H_y \Delta] = -n_1 \left(\frac{\partial_x \hat{\mathbf{n}}}{2} \cdot \frac{\partial_y \hat{\mathbf{n}}}{2} \right), \quad (\text{A8})$$

$$\text{Re}[\Delta^\dagger H_\mu \tau_1 \Delta] = \frac{1}{2}[\hat{\mathbf{n}} \times \partial_x \hat{\mathbf{n}}]_1. \quad (\text{A9})$$

APPENDIX B: GENERAL GROUND STATE

Here, we present the exact solution of the ground state of the general Ginzburg-Landau free energy in the presence of a uniform strain vector $\boldsymbol{\alpha}$. To provide a more intuitive picture of the general ground state, this section first treats the less restrictive case where $\beta_1 \neq \beta_3$ but $\beta'_3 = 0$. We then present the ground state in full generality.

It should be noted, however, that the uniform ground state does not depend on the kinetic terms K and thus we can always renormalize D, G so that $\beta'_3 = 0$.

1. $\beta_1 \neq \beta_3$ and $\beta'_3 = 0$

In the case where $\beta_1 \neq \beta_3$ are positive and $\beta'_3 = 0$, the potential term of the Ginzburg-Landau free energy can be rewritten as

$$V_2 = -|\Delta|^2(\alpha_0 + \alpha_1 n_1 + \alpha_3 n_3), \quad (\text{B1})$$

$$V_4 = \frac{1}{2}|\Delta|^4(1 + \beta_1[n_1]^2 + \beta_3[n_3]^2), \quad (\text{B2})$$

where $\hat{\mathbf{n}}$ is the Bloch vector corresponding to the OP Δ . It is then clear that the potential V is a strongly joint-convex function of $|\Delta|^2$, $|\Delta|^2 n_3$, and $|\Delta|^2 n_1$. Therefore, convex optimization guarantees that the ground state of the uniform system is unique and given by

$$|\Delta|^2 = \alpha_0, \quad n_i = \frac{\alpha_i}{\beta_i \alpha_0}. \quad (\text{B3})$$

Provided that $[n_1]^2 + [n_3]^2 \leq 1$. Conversely, in the case where the above solution is not feasible, i.e., $[n_1]^2 + [n_3]^2 > 1$, the unique ground state is given by

$$|\Delta|^2 = \frac{\alpha_0}{1 - \lambda} \|\Delta\|^2 n_i = \frac{\alpha_i}{\beta_i + \lambda}, \quad (\text{B4})$$

where $\lambda \in [0, 1)$ is chosen so that $[n_1]^2 + [n_3]^2 = 1$. In particular, the ground state corresponds to a Bloch vector $\hat{\mathbf{n}}$ which is in the $\hat{\mathbf{e}}_1$ - $\hat{\mathbf{e}}_3$ plane and thus does not break TRS.

2. Full generality: V is stable and superconducting

In full generality, we still require that the Ginzburg-Landau energy is stable, i.e., the potential term $V \rightarrow \infty$ in the limit where $|\Delta| \rightarrow \infty$. This corresponds to the condition

$$4\beta_3 - \beta_3'^2 > 0. \quad (\text{B5})$$

Similarly, we are only concerned with nontrivial superconducting ground states, which correspond to the condition

$$2\alpha_0\beta_3 - \alpha_3\beta_3' > 0. \quad (\text{B6})$$

Therefore, our general ground-state solution is subject to the two conditions above. The potential term of the Ginzburg-Landau free energy can be rewritten as

$$V_2 = -|\Delta|^2(\alpha_0 + \alpha_1 n_1 + \alpha_3 n_3), \quad (\text{B7})$$

$$V_4 = \frac{1}{2}|\Delta|^4(1 + \beta_1[n_1]^2 + \beta_3[n_3]^2 + \beta_3' n_3). \quad (\text{B8})$$

By our stability condition (B5), the potential term V is a strongly joint-convex function in terms of $|\Delta|^2$, $|\Delta|^2 n_1$, and $|\Delta|^2 n_3$. Therefore, convex optimization guarantees that the ground state of the uniform system is unique and given by

$$\begin{aligned} |\Delta|^2 &= 2 \times \frac{2\alpha_0\beta_3 - \alpha_3\beta_3'}{4\beta_3 - \beta_3'^2} > 0 \|\Delta\|^2 n_3 \\ &= 2 \times \frac{2\alpha_3 - \beta_3'\alpha_0}{4\beta_3 - \beta_3'^2} \|\Delta\|^2 n_1 = \frac{\alpha_1}{\beta_1}. \end{aligned} \quad (\text{B9})$$

Provided that $[n_1]^2 + [n_3]^2 \leq 1$. Conversely, in the case where the above solution is not feasible, i.e., $[n_1]^2 + [n_3]^2 > 1$, the unique ground state is given by

$$\begin{aligned} |\Delta|^2 &= \frac{2}{4(\beta_3 + \lambda) - \beta_3'^2} \\ &\times \left[2(\beta_3 + \lambda)\alpha_0 - \alpha_3\beta_3'^2 + 4\alpha_3 \frac{(\beta_3 + \lambda)\lambda}{\beta_3'} \right] \|\Delta\|^2 n_3 \\ &= 2 \times \frac{2(1 - \lambda)\alpha_3 - \beta_3'\alpha_0}{4(\beta_3 + \lambda) - \beta_3'^2} \|\Delta\|^2 n_1 \\ &= \frac{\alpha_1}{\beta_1 + \lambda}, \end{aligned} \quad (\text{B10})$$

where $\lambda \geq 0$ is chosen so that $[n_1]^2 + [n_3]^2 = 1$. In particular, the ground state corresponds to a Bloch vector \hat{n} which is in the \hat{e}_1 - \hat{e}_3 plane and thus does not break TRS.

APPENDIX C: NARROW DOMAIN WALL CALCULATIONS

In this section, we present detailed calculations of a narrow domain wall between the transition of the TRS states $d - g \rightarrow d + g$. To be more concrete, let us consider the case where $\alpha_3(y) = \underline{\alpha}_3$ is constant, while $\alpha_1(y) = \underline{\alpha}_1 \text{sign}(y)$ changes sign as $y = -\infty \rightarrow +\infty$. The quartic terms are set to $\beta_1 = \beta_3 = \beta > 0$, $\beta_3' = 0$ as before and the strain vector magnitude satisfies $\underline{\alpha} \geq \beta\alpha_0$ so that the uniform ground state at $y \rightarrow \pm\infty$ is denoted by a Bloch vector \hat{n} pointing in the same direction as the strain vector $\underline{\alpha}$ and that the magnitude $|\Delta|^2 = \alpha_0$. Without loss of generality, we shall also assume that $\underline{\alpha}_1, \underline{\alpha}_3 > 0$ so that the angle ψ of the strain vector $\underline{\alpha} \equiv \underline{\alpha}(\sin \psi, 0, \cos \psi)$ satisfies $0 < \psi < \pi/2$ as shown in Fig. 2.

We then calculate the domain wall energy ΔF of possible transition paths as illustrated by the dashed blue and solid green lines in Fig. 2 where the magnitude $|\Delta|^2$ of the OP Δ is assumed to be constant and $= \alpha_0$. In particular, the blue arrow represents a TRS preserving transition, while the green arrow denotes a TRSB transition restricted to a 2D plane at angle ω with respect to the \hat{e}_3 -axis.

1. TRS preserving transition

We shall first consider a TRS preserving transition as described by the dashed blue path in Fig. 2. Notice that we implicitly assumed that $\psi < \pi/2$. If on the other hand, $\psi > \pi/2$, then we would consider the complement path wrapping from underneath the Bloch sphere. Since the transition preserves TRS so that the Bloch vector is in the \hat{e}_1 - \hat{e}_3 plane, we can restrict the azimuthal angle $\phi \equiv 0$ for $y \geq 0$ and $\phi \equiv \pi$ for $y < 0$. Therefore, we can rewrite the Ginzburg-Landau free energy in terms of polar angle θ and average phase χ , i.e., if $y \geq 0$ so that $\theta \geq 0$, then

$$F = V_2 + V_4 + K, \quad (\text{C1})$$

$$V_2 = -|\Delta|^2[\alpha_0 + \underline{\alpha} \cos(\theta - \psi)], \quad (\text{C2})$$

$$V_4 = +\frac{1}{2}|\Delta|^4(1 + \beta), \quad (\text{C3})$$

$$K = \frac{\kappa}{2}|\Delta|^2 \left[\dot{\chi}^2 + \left(\frac{\dot{\theta}}{2} \right)^2 \right]. \quad (\text{C4})$$

It is then clear that $\chi = \text{const}$ and that

$$\frac{\kappa}{2} \frac{\dot{\theta}^2}{2} = \underline{\alpha} \sin(\theta - \psi), \quad (\text{C5})$$

$$\dot{\theta}^2 + \frac{8\underline{\alpha}}{\kappa} \cos(\theta - \psi) = \text{const}. \quad (\text{C6})$$

Using the boundary conditions $\theta \rightarrow \psi$ and $\dot{\theta} \rightarrow 0$ as $y \rightarrow \infty$ and that $\theta = 0$ at $y = 0$, we see that

$$\dot{\theta}^2 = \frac{8\underline{\alpha}}{\kappa} [1 - \cos(\theta - \psi)]. \quad (\text{C7})$$

$$\frac{\dot{\theta}}{2} = -\sqrt{\frac{4\underline{\alpha}}{\kappa}} \sin\left(\frac{\theta - \psi}{2}\right), \quad (\text{C8})$$

$$\theta = \psi - 4 \arctan \left[\tan\left(\frac{\psi}{4}\right) e^{-y/\xi} \right], \quad (\text{C9})$$

where $\xi = \sqrt{\kappa/4\underline{\alpha}}$ is the characteristic length of the domain wall. We can similarly solve for the transition in the case where $y \leq 0$ so that, in general,

$$\theta = \left\{ \psi - 4 \arctan \left[\tan\left(\frac{\psi}{4}\right) e^{-|y|/\xi} \right] \right\}, \quad (\text{C10})$$

$$\phi = \frac{\pi}{2}(1 - \text{sign}y). \quad (\text{C11})$$

We can then calculate the domain wall energy $\Delta F = F - F_0$ for $y \geq 0$ where $F_0 = F[\psi]$ is the Ginzburg-Landau free energy of the uniform ground state, i.e.,

$$\Delta F_{\text{trs}} = \int_0^{+\infty} [F[\chi, \theta, \phi] - F_0] dy \quad (\text{C12})$$

$$= \kappa\alpha_0 \int_0^{+\infty} \left(\frac{\dot{\theta}}{2} \right)^2 dy \quad (\text{C13})$$

$$= \frac{\kappa\alpha_0}{\xi} \int_0^\psi -\sin\left(\frac{\theta - \psi}{2}\right) \frac{d\theta}{2} \quad (\text{C14})$$

$$= \frac{2\kappa\alpha_0}{\xi} \sin^2\left(\frac{\psi}{4}\right). \quad (\text{C15})$$

2. TRSB transition

Let us now consider the special TRSB transition as described by the path with $\omega = \pi/2$ in Fig. 2, so that the polar angle θ of the Bloch vector \hat{n} remains constant and $= \psi < \pi/2$, while the azimuthal angle ϕ twists $\pi \rightarrow 0$. Therefore, we can rewrite the Ginzburg-Landau free energy in terms of azimuthal angle ϕ and average phase χ , i.e., if $y \geq 0$ so that $0 \leq \phi \leq \pi/2$, then

$$F = V_2 + V_4 + K, \quad (\text{C16})$$

$$V_2 = -|\Delta|^2(\alpha_0 + \alpha_1 \sin \psi \cos \phi + \alpha_3 \cos \psi), \quad (\text{C17})$$

$$V_4 = +\frac{1}{2}|\Delta|^4[1 + \beta(1 - \sin^2 \psi \sin^2 \phi)], \quad (\text{C18})$$

$$K = \frac{\kappa}{2}|\Delta|^2 \left[\dot{\chi}^2 + \left(\frac{\dot{\phi}}{2} \right)^2 - \dot{\chi} \dot{\phi} \cos \psi \right]. \quad (\text{C19})$$

By the Euler-Lagrange equations, it is then clear that if the average phase χ satisfies the initial condition $\chi(y \rightarrow -\infty) =$

0, then

$$\chi = \frac{\phi - \pi}{2} \cos \psi. \quad (\text{C20})$$

In particular, the average phase χ changes by $\Delta\chi = -(\pi/2) \cos \psi$ as ϕ twists $\pi \rightarrow 0$. We can similarly solve for ϕ using the boundary condition $\dot{\phi}, \phi \rightarrow 0$ as $y \rightarrow +\infty$ so that

$$\frac{\kappa}{2} \frac{\dot{\phi}}{2} = \sin \phi (\underline{\alpha} - \beta \alpha_0 \cos \phi), \quad (\text{C21})$$

$$\frac{\dot{\phi}}{2} = -\frac{1}{\xi} \sin \left(\frac{\phi}{2} \right) \sqrt{1 - \epsilon \cos^2 \left(\frac{\phi}{2} \right)}, \quad (\text{C22})$$

where $\epsilon = \beta \alpha_0 / \underline{\alpha}$ and $\xi = \sqrt{\kappa / 4\underline{\alpha}}$ is the characteristic length of the domain wall. Notice that by our ground-state discussion (9), the finite strain $\underline{\alpha}$ satisfies $\epsilon \leq 1$ and thus the square root is well defined. We can then solve the first-order differential equation so that

$$\phi = 2 \arccos \left(\frac{1 - \eta}{\sqrt{(1 + \eta)^2 - 4\eta\epsilon}} \right), \quad (\text{C23})$$

where

$$\eta = C \exp \left(-y \frac{\sqrt{1 - \epsilon}}{2\xi} \right), \quad (\text{C24})$$

$$\frac{\pi}{2} = \phi(\eta = C). \quad (\text{C25})$$

We can then calculate the domain wall energy $\Delta F = F - F_0$ for $y \geq 0$ where $F_0 = F[\psi]$ is the Ginzburg-Landau free energy of the uniform ground state, i.e.,

$$\Delta F_{\text{trsb}} = \int_0^{+\infty} [F[\chi, \theta, \phi] - F_0] dy \quad (\text{C26})$$

$$= \kappa \alpha_0 \sin^2 \psi \int_0^{+\infty} \left(\frac{\dot{\phi}}{2} \right)^2 dy \quad (\text{C27})$$

$$= \frac{\kappa \alpha_0}{\xi} \sin^2 \psi \times \int_0^{\pi/2} \sin \left(\frac{\phi}{2} \right) \sqrt{1 - \epsilon \cos^2 \left(\frac{\phi}{2} \right)} \frac{d\phi}{2}. \quad (\text{C28})$$

This can be solved analytically if necessary with the substitution $x = \cos(\phi/2)$. In particular, in the extreme large strain limit $\underline{\alpha} \gg \beta \alpha_0$, the domain wall energy is approximated by

$$\Delta F \approx \frac{2\kappa \alpha_0}{\xi} \sin^2 \psi \sin^2 \left(\frac{\pi}{8} \right). \quad (\text{C29})$$

3. General TRSB transition

Let us finally consider a general TRSB transition as described by the solid green path in Fig. 2. To simplify the problem, we will only consider general TRSB transitions which occur in a 2D plane as shown in Fig. 8, where the transition plane is at an arbitrary angle ω with respect to the vertical plane. If $\omega = 0$, then the transition corresponds to the TRS preserving transition (dashed blue arrow), and if $\omega = \pi/2$,

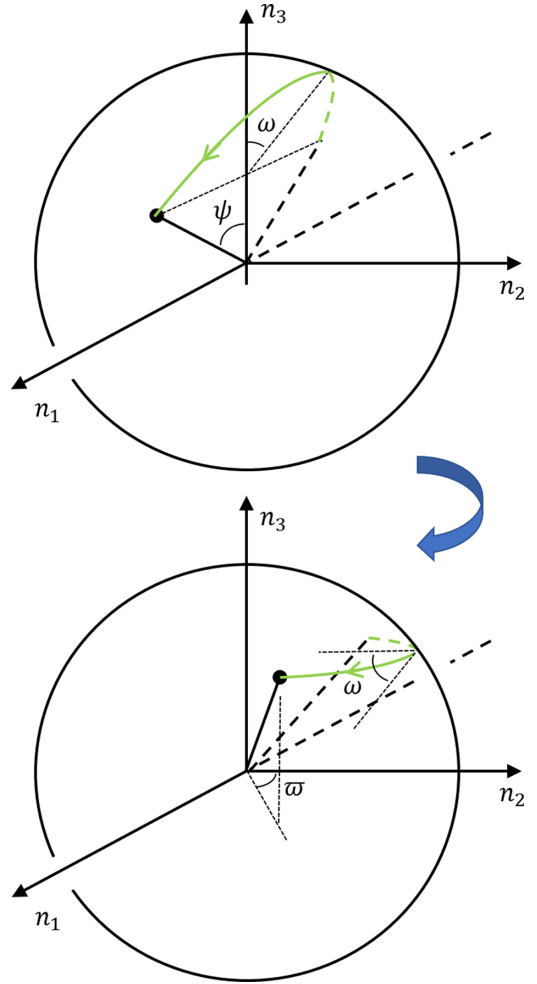


FIG. 8. General TRSB domain wall. The top figure is the Bloch sphere representation of a general TRSB transition through the domain wall $\alpha_1(y) = \underline{\alpha}_1 \text{sign}(y)$. The arrow representing the transition path is assumed to be in a plane at angle ω with respect to the \hat{e}_1 - \hat{e}_3 plane. The bottom figure is the transition rotated of angle ω about the $+x$ -axis in the clockwise direction. All figures are colored in the online version.

then it corresponds to the special TRSB transition. Since the Ginzburg-Landau free energy has a global $SU(2)$ -symmetry, we can rotate the system about the $+x$ -axis of angle ω in the clockwise direction so that the transition occurs in a plane parallel to xy -plane and thus can be parametrized in terms of azimuthal angle ϕ , while the polar angle θ is held fixed, as shown in Fig. 8. This corresponds to using the rotated order parameter $\tilde{\Delta} = U \Delta$ where $U \in SU(2)$ corresponds to the described rotation R . We then rewrite the Ginzburg-Landau free energy so that if $\underline{\alpha} = R \alpha$ is the rotated strain vector and $\varphi \equiv \pi/2 - \phi$ is the azimuthal angle relative to the $+y$ -axis, then

$$F = V_2 + V_4 + K, \quad (\text{C30})$$

$$V_2 = -|\Delta|^2 (\alpha_0 + \underline{\alpha} \cos^2 \theta) - |\Delta|^2 \underline{\alpha} \sin^2 \theta \cos(\varphi - \varpi), \quad (\text{C31})$$

$$V_4 = +\frac{1}{2}|\Delta|^4(1 + \beta) \quad (\text{C32})$$

$$-\frac{1}{2}|\Delta|^4\beta\left(\frac{\sin\theta\cos\theta}{\cos\psi}\right)^2(\cos\varphi - \cos\varpi)^2,$$

$$K = \frac{\kappa}{2}|\Delta|^2\left[\dot{\chi}^2 + \left(\frac{\dot{\psi}}{2}\right)^2 + \dot{\chi}\dot{\psi}\cos\theta\right]. \quad (\text{C33})$$

Here θ is held fixed and ϕ transitions in a manner such that

$$\varphi \equiv \frac{\pi}{2} - \phi = -\varpi \rightarrow 0 \rightarrow \varpi. \quad (\text{C34})$$

As y goes from $-\infty \rightarrow 0 \rightarrow +\infty$, where θ, ϖ are determined by the boundary condition $\alpha \propto \hat{n}(y \rightarrow +\infty)$, i.e.,

$$\sin\psi = \sin\theta\sin\varpi, \quad (\text{C35})$$

$$\cos\psi\cos\omega = \sin\theta\cos\varpi, \quad (\text{C36})$$

$$\cos\psi\sin\omega = \cos\theta. \quad (\text{C37})$$

In particular, $\theta = \pi/2, \varpi = \psi$ for the TRS preserving transition, and $\theta = \psi, \varpi = \pi/2$ for the special TRSB transition.

By the Euler-Lagrange equations, it is then clear that if the global phase χ satisfies the initial condition $\chi(y \rightarrow -\infty) = 0$, then

$$\chi = \frac{\phi}{2}\cos\theta - \frac{1}{2}\left(\frac{\pi}{2} + \varpi\right)\cos\theta. \quad (\text{C38})$$

Hence, the average phase χ changes by $\Delta\chi = -\varpi\cos\theta$ as $y = -\infty \rightarrow \infty$. We can similarly solve for φ so that

$$\frac{\dot{\phi}}{2} = -\frac{1}{\xi}\sin\left(\frac{\varphi - \varpi}{2}\right)$$

$$\times \sqrt{1 - (\epsilon\sin^2\omega)\sin^2\left(\frac{\varphi - \varpi}{2} + \varpi\right)}, \quad (\text{C39})$$

where $\epsilon = \beta\alpha_0/\alpha \leq 1$ and $\xi = \sqrt{\kappa/4\alpha}$ is the characteristic length of the domain wall. It should be noted that the equation can be solved analytically for arbitrary $\epsilon \leq 1$, albeit in implicit form, i.e., $f(\varphi) = y$ for some function f . It should be noted that the explicit form $\varphi = \varphi(y)$ is not necessary to compute the domain wall energy ΔF . Indeed, we have

$$\Delta F = \int_0^{+\infty} [F[\chi, \theta, \phi] - F_0] dy \quad (\text{C40})$$

$$= \kappa\alpha_0\sin^2\theta \int_0^{+\infty} \left(\frac{\dot{\phi}}{2}\right)^2 dy \quad (\text{C41})$$

$$= \frac{\kappa\alpha_0}{\xi}\sin^2\theta$$

$$\times \int_0^{\varpi/2} \sin x \sqrt{1 - (\epsilon\sin^2\omega)\sin^2(\varpi - x)} dx. \quad (\text{C42})$$

In the extreme large strain limit $\alpha \gg \beta\alpha_0$, the domain wall energy is approximated by

$$\Delta F \approx \frac{2\kappa\alpha_0}{\xi}\sin^2\theta\sin^2\left(\frac{\varpi}{4}\right). \quad (\text{C43})$$

APPENDIX D: FULLY SELF-CONSISTENT EQUATIONS

In this section, we derive the full self-consistency field equations (SCFs) for the full Hamiltonian $H_{\text{full}} = H_0 + H_1$ defined in Eqs. (12) and (13). Let us first write the corresponding BCS Hamiltonian H as

$$H = \sum_{\vec{r}', \vec{r}, s} \mathcal{T}(\vec{r}', \vec{r}) c_{\vec{r}'s}^\dagger c_{\vec{r}s}$$

$$+ \sum_{\vec{r}', \vec{r}} (\Delta_{\vec{r}', \vec{r}} c_{\vec{r}'\uparrow}^\dagger c_{\vec{r}\downarrow}^\dagger + \text{H.c.}) \quad (\text{D1})$$

$$= [c_\uparrow^\dagger \quad c_\downarrow] \hat{H} \begin{bmatrix} c_\uparrow \\ c_\downarrow \end{bmatrix}, \quad \hat{H} = \begin{bmatrix} \mathcal{T} & \Delta \\ \Delta^\dagger & -\bar{\mathcal{T}} \end{bmatrix}. \quad (\text{D2})$$

To simplify notation, let us introduce the notation $1_{\vec{r}} = |\vec{r}\rangle\langle\vec{r}|$ for the projection operator and the one-particle density matrices (**1-pdms**) [45] of the BCS Hamiltonian H , i.e.,

$$\gamma(\vec{r}', \vec{r}) = \langle c_{\vec{r}'\uparrow}^\dagger c_{\vec{r}\uparrow} \rangle = \langle c_{\vec{r}'\downarrow}^\dagger c_{\vec{r}\downarrow} \rangle, \quad (\text{D3})$$

$$\alpha(\vec{r}', \vec{r}) = \langle c_{\vec{r}'\downarrow} c_{\vec{r}\uparrow} \rangle = -\langle c_{\vec{r}'\uparrow} c_{\vec{r}\downarrow} \rangle. \quad (\text{D4})$$

The Hartree-Fock energy $\langle H_{\text{full}} \rangle = \langle H_0 \rangle + \langle H_1 \rangle$ can then be computed via Wick's theorem so that

$$\langle H_0 \rangle = 2\text{tr}(\mathcal{T}\gamma), \quad (\text{D5})$$

$$\langle H_1 \rangle = -2 \sum_{\tau=d,g} \lambda_\tau \sum_{\vec{r}} \text{tr}(2f_\tau \alpha^\dagger 1_{\vec{r}} \alpha f_\tau^\dagger 1_{\vec{r}})$$

$$+ f_\tau^\dagger \gamma 1_{\vec{r}} \gamma f_\tau 1_{\vec{r}} + \gamma 1_{\vec{r}} f_\tau^\dagger \gamma f_\tau 1_{\vec{r}}. \quad (\text{D6})$$

The self-consistency field equations (SCFs) can then be derived from extremizing the variational free energy $\delta F \equiv \delta \langle H_{\text{full}} \rangle - T\delta S_H = 0$ and written in operator form

$$\mathcal{T} = t - \sum_{\tau=d,g} \lambda_\tau \sum_{\vec{r} \in \Lambda} [(f_\tau 1_{\vec{r}} f_\tau^\dagger \gamma 1_{\vec{r}} + \text{H.c.})$$

$$+ 1_{\vec{r}} f_\tau^\dagger \gamma f_\tau 1_{\vec{r}} + f_\tau 1_{\vec{r}} \gamma 1_{\vec{r}} f_\tau^\dagger], \quad (\text{D7})$$

$$\Delta = -2 \sum_{\tau=d,g} \lambda_\tau \sum_{\vec{r}} (f_\tau 1_{\vec{r}} \alpha f_\tau^\dagger 1_{\vec{r}} + \text{tr}), \quad (\text{D8})$$

where tr implies the transpose term $= 1_{\vec{r}} f_\tau^\dagger \alpha 1_{\vec{r}} f_\tau = 1_{\vec{r}} \alpha f_\tau^\dagger 1_{\vec{r}} f_\tau$, and we used the fact that α, f_τ are symmetric, i.e., $\alpha^T = \alpha, f_\tau^T = f_\tau$. The proposed format of writing the SCFs in operator form has the advantage of working in any basis set, and in particular, we can work in real space $|\vec{r}\rangle$ or momentum space $|\vec{k}\rangle$. This will simplify our algebra later on. The corresponding BdG equations can similarly be written as

$$\gamma = un_E u^\dagger + \bar{v}(1 - n_E)v^T, \quad (\text{D9})$$

$$\alpha = -\frac{1}{2} \left[u \tanh\left(\frac{\beta E}{2}\right) v^\dagger + \text{transpose} \right], \quad (\text{D10})$$

where n_E is the diagonal matrix with entries of the Fermi distribution $n_E = (e^{\beta E} + 1)^{-1}$ and u, v are chosen so that the following unitary matrix W diagonalizes the first quantized Hamiltonian \hat{H} , i.e.,

$$\hat{H} = W \begin{bmatrix} E & 0 \\ 0 & -E \end{bmatrix} W^\dagger, \quad W = \begin{bmatrix} u & -\bar{v} \\ v & \bar{u} \end{bmatrix}. \quad (\text{D11})$$

Notice that the BdG Eqs. (D9) can also be written in the more compact form [45]

$$\Gamma = W \begin{bmatrix} n_E & 0 \\ 0 & 1 - n_E \end{bmatrix} W^\dagger, \quad (\text{D12})$$

where

$$\Gamma = \begin{bmatrix} \gamma & \alpha \\ \alpha^\dagger & 1 - \bar{\gamma} \end{bmatrix} = \frac{1}{e^{\beta \hat{H}} + 1}. \quad (\text{D13})$$

Uniform system in momentum space

The full SCFs can be further simplified in a uniform system, so that the 1-pdms γ , α (D3), hopping matrix t and form factors f_τ are diagonalized in \vec{k} -space. In particular,

$$\gamma(\vec{k}) = \langle c_{\vec{k}\uparrow}^\dagger c_{\vec{k}\uparrow} \rangle = \langle c_{\vec{k}\downarrow}^\dagger c_{\vec{k}\downarrow} \rangle, \quad (\text{D14})$$

$$\alpha(\vec{k}) = \langle c_{-\vec{k}\downarrow} c_{\vec{k}\uparrow} \rangle = -\langle c_{\vec{k}\uparrow} c_{-\vec{k}\downarrow} \rangle. \quad (\text{D15})$$

In this case, the SCFs (D7) are reduced to

$$\begin{aligned} \mathcal{T}(\vec{k}) &= t(\vec{k}) - \sum_{\tau=d,g} \lambda_\tau (f_\tau(\vec{k}) \llbracket f_\tau \gamma \rrbracket + \text{H.c.}) \\ &\quad + \llbracket \gamma |f_\tau|^2 \rrbracket + |f_\tau(\vec{k})|^2 \llbracket \gamma \rrbracket, \end{aligned} \quad (\text{D16})$$

$$\Delta(\vec{k}) = -4 \sum_{\tau=d,g} \lambda_\tau f_\tau(\vec{k}) \llbracket \alpha f_\tau^\dagger \rrbracket, \quad (\text{D17})$$

where we use the notation $\llbracket \cdot \rrbracket$ as the average value summed over \vec{k} -space, i.e.,

$$\llbracket h \rrbracket = \int_{(-\pi, \pi]^2} \frac{d^2 \vec{k}}{(2\pi)^2} h(\vec{k}). \quad (\text{D18})$$

Notice that the specific form of our Δ -function (D16), i.e., $\Delta(\vec{k}) = D f_d(\vec{k}) + G f_g(\vec{k})$ for complex constants D, G implies that the SCFs indeed yield a two-component OP theory. Similarly, the BdG equations are reduced to

$$\begin{aligned} \gamma(\vec{k}) &= \frac{1}{2} \left(1 + \frac{\mathcal{T}(\vec{k})}{E(\vec{k})} \right) n(\vec{k}) \\ &\quad + \frac{1}{2} \left(1 - \frac{\mathcal{T}(\vec{k})}{E(\vec{k})} \right) [1 - n(\vec{k})], \end{aligned} \quad (\text{D19})$$

$$\alpha(\vec{k}) = -\frac{\Delta(\vec{k})}{2E(\vec{k})} \tanh \left(\frac{\beta E(\vec{k})}{2} \right), \quad (\text{D20})$$

where $n(\vec{k}) = (e^{\beta E(\vec{k})} + 1)^{-1}$ is the Fermi distribution of the Bogoliubov quasiparticles with dispersion relation

$$E(\vec{k}) = \sqrt{\mathcal{T}(\vec{k})^2 + |\Delta(\vec{k})|^2}. \quad (\text{D21})$$

APPENDIX E: $\nabla \cdot \mathbf{J} = 0$ IN BCS THEORY

Let $H[\psi]$ denote the BCS Hamiltonian with parameters $\psi = (\xi, \Delta)$. Let the particular choice of parameter φ be such that $H[\varphi]$ satisfies the *full* self-consistency equations with respect to the full Hamiltonian H_{full} , i.e.,

$$\left. \frac{\partial}{\partial \psi} \right|_{\psi=\varphi} \langle H_{\text{full}} \rangle_\psi = \frac{1}{\beta} \left. \frac{\partial}{\partial \psi} \right|_{\psi=\varphi} S[\psi], \quad (\text{E1})$$

where $S[\psi]$ is the von Neumann entropy of $H[\psi]$ defined by $S = -\text{tr}(\rho \log \rho)$ where ρ is the Gibbs distribution of the BCS Hamiltonian $H[\psi]$, and $\langle \cdot \cdot \rangle_\psi$ is the thermal average at temperature T with respect to the BCS Hamiltonian $H[\psi]$.

We shall subsequently show that at any temperature and every lattice site \vec{r} , the charge density $\rho(\vec{r})$ is constant in BCS theory, i.e.,

$$\left. \frac{\partial \rho(\vec{r})}{\partial t} \right|_{t=0} = 0. \quad (\text{E2})$$

As a corollary, we can apply the continuity equation $\partial_t \rho(\vec{r}) = \nabla \cdot \mathbf{J}(\vec{r}) \equiv \sum_{\vec{r}'} \mathbf{J}(\vec{r}', \vec{r})$ to obtain

$$\langle \nabla \cdot \mathbf{J}(\vec{r}) \rangle_\varphi \equiv \sum_{\vec{r}' \in \Lambda} \langle \mathbf{J}(\vec{r}', \vec{r}) \rangle_\varphi = 0. \quad (\text{E3})$$

Indeed, let us introduce the notation for gauge transformation at lattice site \vec{r} , i.e., if M is an operator, e.g., the full Hamiltonian H_{full} or the BCS Hamiltonian $H[\psi]$, then define

$$M(s) = e^{is\rho(\vec{r})} A e^{-is\rho(\vec{r})}, \quad s \in \mathbb{R}. \quad (\text{E4})$$

In this case, notice that

$$H[\varphi](s) = H[\varphi(s)], \quad (\text{E5})$$

where $\varphi(s)$ denote the parameters

$$\mathcal{T}(\vec{r}'', \vec{r}') (s) = \mathcal{T}(\vec{r}'', \vec{r}') e^{is[\delta(\vec{r}'', \vec{r}) - \delta(\vec{r}', \vec{r})]}, \quad (\text{E6})$$

$$\Delta(\vec{r}'', \vec{r}') (s) = \Delta(\vec{r}'', \vec{r}') e^{is[\delta(\vec{r}'', \vec{r}) + \delta(\vec{r}', \vec{r})]}. \quad (\text{E7})$$

Also notice that the BCS partition function $Z[\varphi(s)]$ is independent of s since the trace is invariant under unitary gauge transforms and thus

$$\left\langle \frac{\partial H_{\text{full}}(s)}{\partial s} \right\rangle_{\varphi_s} = \frac{1}{Z_\varphi} \text{tr} \left(e^{-\beta H[\varphi_s]} \frac{\partial H_{\text{full}}(s)}{\partial s} \right) \quad (\text{E8})$$

$$= +\frac{1}{Z_\varphi} \frac{\partial}{\partial s} \text{tr} [e^{-\beta H[\varphi_s]} H_{\text{full}}(s)] \quad (\text{E9})$$

$$- \frac{1}{Z_\varphi} \text{tr} \left(H_{\text{full}}(s) \frac{\partial}{\partial s} e^{-\beta H[\varphi_s]} \right). \quad (\text{E10})$$

The first term is = 0 since the trace is invariant under unitary transforms. Setting $s = 0$, we see that

$$- \left\langle \frac{\partial H_{\text{full}}(s)}{\partial s} \right|_{s=0} \Big|_\varphi = \frac{1}{Z_\varphi} \text{tr} \left(H_{\text{full}} \frac{\partial}{\partial s} \Big|_{s=0} e^{-\beta H[\varphi_s]} \right) \quad (\text{E11})$$

$$= \frac{\partial}{\partial s} \Big|_{s=0} \frac{1}{Z_\varphi} \text{tr} (H_{\text{full}} e^{-\beta H[\varphi_s]}) \quad (\text{E12})$$

$$= \frac{\partial}{\partial s} \Big|_{s=0} \langle H_{\text{full}} \rangle_{\varphi_s} \quad (\text{E13})$$

$$= \frac{\partial \varphi_s}{\partial s} \Big|_{s=0} \frac{\partial}{\partial \psi} \Big|_{\psi=\varphi} \langle H_{\text{full}} \rangle_\psi \quad (\text{E14})$$

$$= \frac{1}{\beta} \frac{\partial \varphi_s}{\partial s} \Big|_{s=0} \frac{\partial}{\partial \psi} \Big|_{\psi=\varphi} S[\psi] \quad (\text{E15})$$

$$= \frac{1}{\beta} \frac{\partial}{\partial s} \Big|_{s=0} S[\varphi_s]. \quad (\text{E16})$$

Notice that $S[\varphi_s]$ is independent of s since the trace is invariant under unitary gauge transforms. Hence, the right-hand side is $= 0$ and thus we arrive at the statement

$$\left\langle \frac{\partial \rho(\vec{r})}{\partial t} \Big|_{t=0} \right\rangle_{\varphi} = - \left\langle \frac{\partial H_{\text{full}}(s)}{\partial s} \Big|_{s=0} \right\rangle_{\varphi} = 0. \quad (\text{E17})$$

-
- [1] C. Platt, R. Thomale, C. Honerkamp, S.-C. Zhang, and W. Hanke, Mechanism for a pairing state with time-reversal symmetry breaking in iron-based superconductors, *Phys. Rev. B* **85**, 180502(R) (2012).
- [2] A. P. Mackenzie, T. Scaffidi, C. W. Hicks, and Y. Maeno, Even odder after twenty-three years: The superconducting order parameter puzzle of Sr_2RuO_4 , *npj Quantum Mater.* **2**, 40 (2017).
- [3] S. A. Kivelson, A. C. Yuan, B. J. Ramshaw, and R. Thomale, A proposal for reconciling diverse experiments on the superconducting state in Sr_2RuO_4 , *npj Quantum Mater.* **5**, 43 (2020).
- [4] A. T. Rømer, A. Kreisel, M. A. Müller, P. J. Hirschfeld, I. M. Eremin, and B. M. Andersen, Theory of strain-induced magnetic order and splitting of T_c and T_{rsb} in Sr_2RuO_4 , *Phys. Rev. B* **102**, 054506 (2020).
- [5] A. T. Rømer, P. J. Hirschfeld, and B. M. Andersen, Superconducting state of Sr_2RuO_4 in the presence of longer-range Coulomb interactions, [arXiv:2101.06972](https://arxiv.org/abs/2101.06972).
- [6] R. Willa, M. Hecker, R. M. Fernandes, and J. Schmalian, Inhomogeneous time-reversal symmetry breaking in Sr_2RuO_4 , *Phys. Rev. B* **104**, 024511 (2021).
- [7] A. Pustogow, Y. Luo, A. Chronister, Y.-S. Su, D. A. Sokolov, F. Jerzembeck, A. P. Mackenzie, C. W. Hicks, N. Kikugawa, S. Raghu *et al.*, Constraints on the superconducting order parameter in Sr_2RuO_4 from oxygen-17 nuclear magnetic resonance, *Nature (London)* **574**, 72 (2019).
- [8] K. Ishida, M. Manago, K. Kinjo, and Y. Maeno, Reduction of the 17O Knight shift in the superconducting state and the heat-up effect by NMR pulses on Sr_2RuO_4 , *J. Phys. Soc. Jpn.* **89**, 034712 (2020).
- [9] A. Chronister, A. Pustogow, N. Kikugawa, D. A. Sokolov, F. Jerzembeck, C. W. Hicks, A. P. Mackenzie, E. D. Bauer, and S. E. Brown, Evidence for even parity unconventional superconductivity in Sr_2RuO_4 , *PNAS* **118**, e2025313118 (2021).
- [10] S. Ghosh, A. Shekhter, F. Jerzembeck, N. Kikugawa, D. A. Sokolov, M. Brando, A. P. Mackenzie, C. W. Hicks, and B. J. Ramshaw, Thermodynamic evidence for a two-component superconducting order parameter in Sr_2RuO_4 , *Nat. Phys.* **17**, 199 (2021).
- [11] S. Benhabib, C. Lupien, I. Paul, L. Berges, M. Dion, M. Nardone, A. Zitouni, Z. Q. Mao, Y. Maeno, A. Georges *et al.*, Ultrasound evidence for a two-component superconducting order parameter in Sr_2RuO_4 , *Nat. Phys.* **17**, 194 (2021).
- [12] G. M. Luke, Y. Fudamoto, K. M. Kojima, M. I. Larkin, J. Merrin, B. Nachumi, Y. J. Uemura, Y. Maeno, Z. Q. Mao, Y. Mori *et al.*, Time-reversal symmetry-breaking superconductivity in Sr_2RuO_4 , *Nature (London)* **394**, 558 (1998).
- [13] J. Xia, Y. Maeno, P. T. Beyersdorf, M. M. Fejer, and A. Kapitulnik, High Resolution Polar Kerr Effect Measurements of Sr_2RuO_4 : Evidence for Broken Time-Reversal Symmetry in the Superconducting State, *Phys. Rev. Lett.* **97**, 167002 (2006).
- [14] F. Kidwingira, J. D. Strand, D. J. Van Harlingen, and Y. Maeno, Dynamical superconducting order parameter domains in Sr_2RuO_4 , *Science* **314**, 1267 (2006).
- [15] V. Grinenko, S. Ghosh, R. Sarkar, J.-C. Orain, A. Nikitin, M. Elender, D. Das, Z. Guguchia, F. Brückner, M. E. Barber *et al.*, Split superconducting and time-reversal symmetry-breaking transitions in Sr_2RuO_4 under stress, *Nat. Phys.* **17**, 748 (2021).
- [16] Y.-S. Li, R. Borth, C. W. Hicks, A. P. Mackenzie, and M. Nicklas, Heat-capacity measurements under uniaxial pressure using a piezo-driven device, *Rev. Sci. Instrum.* **91**, 103903 (2020).
- [17] V. Grinenko, D. Das, R. Gupta, B. Zinkl, N. Kikugawa, Y. Maeno, C. W. Hicks, H.-H. Klauss, M. Sigrist, and R. Khasanov, Unsplit superconducting and time reversal symmetry breaking transitions in Sr_2RuO_4 under hydrostatic pressure and disorder, *Nat. Commun.* **12**, 3920 (2021).
- [18] J. Jang, D. G. Ferguson, V. Vakaryuk, R. Budakian, S. B. Chung, P. M. Goldbart, and Y. Maeno, Observation of half-height magnetization steps in Sr_2RuO_4 , *Science* **331**, 186 (2011).
- [19] A. J. Leggett and Y. Liu, Symmetry Properties of Superconducting Order Parameter in Sr_2RuO_4 , *J. Supercond. Novel Magn.* **34**, 1647 (2020).
- [20] X. Cai, B. M. Zakrzewski, Y. A. Ying, H.-Y. Kee, M. Sigrist, J. E. Ortmann, W. Sun, Z. Mao, and Y. Liu, Magnetoresistance oscillation study of the half-quantum vortex in doubly connected mesoscopic superconducting cylinders of Sr_2RuO_4 , [arXiv:2010.15800](https://arxiv.org/abs/2010.15800).
- [21] Note that the same sort of analysis can be applied to a domain wall across which $\alpha_3(y)$ changes sign with $\alpha_1 = \text{constant}$, e.g., between a region of $D + g$ pairing (indicating dominant D and subdominant g) to $d + G$ pairing (dominant G).
- [22] D. S. Jin, S. A. Carter, B. Ellman, T. F. Rosenbaum, and D. G. Hinks, Uniaxial-Stress Anisotropy of the Double Superconducting Transition in UPt_3 , *Phys. Rev. Lett.* **68**, 1597 (1992).
- [23] G. M. Luke, A. Keren, L. P. Le, W. D. Wu, Y. J. Uemura, D. A. Bonn, L. Taillefer, and J. D. Garrett, Muon Spin Relaxation in UPt_3 , *Phys. Rev. Lett.* **71**, 1466 (1993).
- [24] E. R. Schemm, W. J. Gannon, C. M. Wishne, W. P. Halperin, and A. Kapitulnik, Observation of broken time-reversal symmetry in the heavy-fermion superconductor UPt_3 , *Science* **345**, 190 (2014).
- [25] T. Yamashita, Y. Shimoyama, Y. Haga, T. D. Matsuda, E. Yamamoto, Y. Onuki, H. Sumiyoshi, S. Fujimoto, A. Levchenko, T. Shibauchi *et al.*, Colossal thermomagnetic response in the exotic superconductor URu_2Si_2 , *Nat. Phys.* **11**, 17 (2015).
- [26] E. R. Schemm, R. E. Baumbach, P. H. Tobash, F. Ronning, E. D. Bauer, and A. Kapitulnik, Evidence for broken time-reversal symmetry in the superconducting phase of URu_2Si_2 , *Phys. Rev. B* **91**, 140506(R) (2015).

- [27] I. M. Hayes, D. S. Wei, T. Metz, J. Zhang, Y. S. Eo, S. Ran, S. R. Saha, J. Collini, N. P. Butch, D. F. Agterberg, A. Kapitulnik, and J. Paglione, Weyl Superconductivity in UTe_2 , [arXiv:2002.02539](#).
- [28] K. Matano, M. Kriener, K. Segawa, Y. Ando, and G.-Q. Zheng, Spin-rotation symmetry breaking in the superconducting state of $\text{Cu}_x\text{Bi}_2\text{Se}_3$, [Nat. Phys.](#) **12**, 852 (2016).
- [29] L. Fu, Odd-parity topological superconductor with nematic order: Application to $\text{Cu}_x\text{Bi}_2\text{Se}_3$, [Phys. Rev. B](#) **90**, 100509(R) (2014).
- [30] R. M. Fernandes, A. V. Chubukov, and J. Schmalian, What drives nematic order in iron-based superconductors? [Nat. Phys.](#) **10**, 97 (2014).
- [31] V. Grinenko, R. Sarkar, K. Kihou, C. H. Lee, I. Morozov, S. Aswartham, B. Büchner, P. Chekhonin, W. Skrotzki, K. Nenkov *et al.*, Superconductivity with broken time-reversal symmetry inside a superconducting s -wave state, [Nat. Phys.](#) **16**, 789 (2020).
- [32] T. Böhm, A. F. Kemper, B. Moritz, F. Kretzschmar, B. Muschler, H. M. Eiter, R. Hackl, T. P. Devereaux, D. J. Scalapino, and H.-H. Wen, Balancing Act: Evidence for a Strong Subdominant d -Wave Pairing Channel in $\text{Ba}_{0.6}\text{K}_{0.4}\text{Fe}_2\text{As}_2$, [Phys. Rev. X](#) **4**, 041046 (2014).
- [33] G. E. Volovik and V. P. Mineev, Line and point singularities in superfluid ^3He , [JETP Lett.](#) **24**, 562 (1976).
- [34] M. Sigrist, T. M. Rice, and K. Ueda, Low-Field Magnetic Response of Complex Superconductors, [Phys. Rev. Lett.](#) **63**, 1727 (1989).
- [35] S. B. Chung, H. Bluhm, and E.-A. Kim, Stability of Half-Quantum Vortices in $p_x + ip_y$ Superconductors, [Phys. Rev. Lett.](#) **99**, 197002 (2007).
- [36] F. Wu and I. Martin, Majorana Kramers pair in a nematic vortex, [Phys. Rev. B](#) **95**, 224503 (2017).
- [37] S. B. Etter, W. Huang, and M. Sigrist, Half-quantum vortices on c -axis domain walls in chiral p -wave superconductors, [New J. Phys.](#) **22**, 093038 (2020).
- [38] E. Babaev, Vortices with Fractional Flux in Two-Gap Superconductors and in Extended Faddeev Model, [Phys. Rev. Lett.](#) **89**, 067001 (2002).
- [39] E. Babaev, J. Jäykkä, and M. Speight, Magnetic Field Delocalization and Flux Inversion in Fractional Vortices in Two-Component Superconductors, [Phys. Rev. Lett.](#) **103**, 237002 (2009).
- [40] M. H. Fischer and E. Berg, Fluctuation and strain effects in a chiral p -wave superconductor, [Phys. Rev. B](#) **93**, 054501 (2016).
- [41] Y. Yu and S. Raghu, Effect of strain inhomogeneity on a chiral p -wave superconductor, [Phys. Rev. B](#) **100**, 094517 (2019).
- [42] M. Hecker and J. Schmalian, Vestigial nematic order and superconductivity in the doped topological insulator $\text{Cu}_x\text{Bi}_2\text{Se}_3$, [npj Quantum Mater.](#) **3**, 26 (2018).
- [43] C.-w. Cho, J. Shen, J. Lyu, O. Atanov, Q. Chen, S. H. Lee, Y. S. Hor, D. J. Gawryluk, E. Pomjakushina, M. Bartkowiak, M. Hecker, J. Schmalian, and R. Lortz, Z_3 -vestigial nematic order due to superconducting fluctuations in the doped topological insulators $\text{Nb}_x\text{Bi}_2\text{Se}_3$ and $\text{Cu}_x\text{Bi}_2\text{Se}_3$, [Nat. Commun.](#) **11**, 3056 (2020).
- [44] K. D. Nelson, Z. Q. Mao, Y. Maeno, and Y. Liu, Odd-parity superconductivity in Sr_2RuO_4 , [Science](#) **306**, 1151 (2004).
- [45] V. Bach, E. H. Lieb, and J. P. Solovej, Generalized Hartree-Fock theory and the Hubbard model, [J. Stat. Phys.](#) **76**, 3 (1994).